WANL-PR(P)-005
CR 54232

DETERMINATION OF THE WELDABILITY AND ELEVATED TEMPERATURE STABILITY OF REFRACTORY METAL ALLOYS

Fifth Quarterly Report

by
G. G. Lessmann and D. R. Stoner

prepared for
NATIONAL AERONAUTICS AND SPACE ADMINISTRATION
LEWIS RESEARCH CENTER
UNDER CONTRACT NAS3-2540

Astronuclear Laboratory
Westinghouse Electric Corporation

Astronuclear

WANL-PR-(P)-005

CR 54232

DETERMINATION OF THE WELDABILITY AND ELEVATED TEMPERATURE STABILITY OF REFRACTORY METAL ALLOYS

by

G. G. Lessmann

and

D. R. Stoner

FIFTH QUARTERLY REPORT

Covering the Period

June 21, 1964 to September 20, 1964

Prepared For

NATIONAL AERONAUTICS AND SPACE ADMINISTRATION
Contract NAS 3-2540

Technical Management
Paul E. Moorhead
NASA - Lewis Research Center

Astronuclear Laboratory
Westinghouse Electric Corporation
Pittsburgh 36, Pa.

Astronuclear

FOREWORD

This report describes work accomplished under Contract NAS 3-2540 during the period June 21, 1964 to September 20, 1964. This program is being administered by R. T. Begley of the Astronuclear Laboratory, Westinghouse Electric Corporation. G. G. Lessmann and D. R. Stoner performed the experimental investigations.

P. E. Moorhead of the National Aeronautics and Space Administration, is Technical Manager of this program.

Astronuclear

TABLE OF CONTENTS

LIST OF FIGURES

LIST OF FIGURES
(continued)

Astronuclear

LIST OF TABLES

I. INTRODUCTION

This is the Fifth Quarterly Progress Report describing work accomplished under Contract NAS 3-2540. The objective of this program is to determine the weldability and long time elevated temperature stability of promising refractory metal alloys in order to determine those most suitable for use in advanced alkali-metal space electric power systems. A detailed discussion of the program and program objectives was presented in the First Quarterly Report. Alloys included in this investigation are listed in Table 1.

Process and test controls employed throughout this program emphasize the important influence of interstitial elements on the properties of refractory metal alloys. Stringent process and test procedures are required, including continuous monitoring of the TIG weld chamber atmosphere, electron beam welding at low pressures, aging in furnaces employing hydrocarbon free pumping systems providing pressures less than 10^{-8} torr, and chemical sampling following successive stages of the evaluation for verification of these process controls.

Equipment requirements and set-up, and procedures for welding and testing, have been described in previous progress reports. Any improvements in processes, changes in procedures, or additional processes and procedures are described in this report.

TABLE 1 - Alloys Included in the Weldability and Thermal Stability Evaluations

Alloy	Nominal Composition Weight Percent
AS-55	Cb-5W-1Zr-0.2Y-0.06C
B-66	Cb-5Mo-5V-1Zr
C-129Y	Cb-10W-10Hf+Y
Cb-752	Cb-10W-2.5Zr
D-43	Cb-10W-1Zr-0.1C
FS-85	Cb-27Ta-10W-1Zr
SCb-291	Cb-10W-10Ta
T-111	Ta-8W-2Hf
T-222	Ta-9.6W-2.4Hf-0.01C
Ta-10W	Ta-10W
W-25Re	W-25RE
W	Unalloyed
Sylvania "A"	W-0.5Hf-0.02C

Note: All alloys to be from arc-cast and/or electron beam melted material except Sylvania "A"

II. SUMMARY

The delivery status of the thirteen alloys included in this program is shown in Table 2. Orders for eleven of these have been filled.

TIG sheet butt welds for the weld parameter study have been completed for all of the available alloys except W-25Re and unalloyed tungsten. Special handling and welding techniques are required for the W-25Re, unalloyed tungsten, and Sylvania "A", hence welding of these has been deferred. With the exception of T-111 and AS-55 which have not yet been bend tested, test data for the remaining alloys are presented in this report. A summary of current bend test results is given in Figure 1.

EB sheet butt welds for the weld parameter study have been completed for all available alloys except AS-55 and unalloyed tungsten. Bend test data on two additional alloys, D-43 and W-25Re, are presented in this report. Previous reports presented bend test data on Ta-10W, FS-85, SCb-291, and Cb-752.

Unexpectedly high bend ductile-brittle transition temperatures (in some cases exceeding 1000°F using a 4t bend radius) have been obtained for the W-25Re EB welds. A review of this problem has been undertaken. Welds are being examined for contamination, segregation, or unusual structure, the effect and magnitude of residual stresses, and for weld, heat affected zone or base metal defects.

A thorough evaluation of the high vacuum annealing furnace performance under simulated long time aging conditions was made. A dummy load of refractory metal alloys, mostly in sheet form, was annealed at 3200°F for 500 hours. For this run the furnace was baked out at 450°F for 20 hours below 5×10^{-6} torr pressure before furnace start-up. The system was pumped by a sputter ion pump with auxiliary titanium sublimation pumping. Total and partial pressures were monitored by a Bayard-Alpert type nude ion gage, ion pump current, and a Veeco GA-3 magnetic sector residual gas analyzer. A high initial hydrogen load was observed during the first five hours of furnace operation. After this, carbon monoxide was the principal gas load component. Constituent partial pressures as well as total pressures dropped steadily throughout the test run. Titanium sublimation pumping was least effective in improving the pumping of hydrogen and moisture and most effective in improving the pumping of inert gases.

Latex natural rubber gloves were evaluated for use on the TIG weld chamber and were found to be inferior to neoprene. They were subject to decomposition under vacuum bakeout (150-200°F) as evidenced by an unidentified tacky film which condensed on the cooler weld box wall during bakeout. Oxygen permeability of the natural rubber gloves was an order of magnitude worse than for neoprene while moisture permeability was about the same.

TABLE 2 - Alloy Procurement and Delivery Schedule

Alloy	Approval	Quotation	Ordered	Shipping Date	Actual Delivery			Supplier
					Sheet	Plate	Wire	
AS-55	8/12/63	10/1/63	1/29/64	5/1/64	8/25/64	---[3]	---[3]	Gen. Electric (Cleveland)
B-66	8/12/63	8/19/63	8/29/63	10/18/63	3/3/64	3/3/64	11/8/63	Westinghouse
C-129Y	8/12/63	9/20/63	10/2/63	11/30/63	12/24/64	3/13/64	3/13/64	Wah Chang
Cb-752	8/12/63	9/19/63	10/21/63	11/30/63	12/31/63	12/18/63	12/31/63	Haynes
D-43	8/12/63	8/17/63	9/3/63	11/8/63	11/15/63	10/18/63	2/12/64	Du Pont
FS-85	8/12/63	8/12/63	8/22/63	1/30/64	3/6/64	1/6/64	3/7/64	Fansteel[1]
SCb-291	8/12/63	9/17/63	10/2/63	1/30/64	1/9/64	1/8/64	12/6/63	Fansteel
T-111	8/12/63	8/16/63 6/25/64[2] 6/25/64	9/27/63 8/5/64 ---[5]	10/28/63 9/28/64 ---[5]	---[4] 11/17/64 ---[4]	12/31/63 ---[4] ---[4]	---[4] ---[4] 8/14/64	NRC Wah Chang Westinghouse
T-222	2/28/64	6/29/64[2]	7/20/64	9/28/64	12/16/64	12/16/64		Wah Chang
Ta-10W	8/12/63	8/12/63	8/22/63	9/30/63	10/21/63	10/3/63	10/17/63	Fansteel
W-25Re	8/12/63	11/26/63	2/1/64	4/1/64	5/29/64	---[3]	---[3]	Wah Chang
W	2/28/64	2/19/64	4/16/64	6/15/64	7/30/64	---[3]	---[3]	Universal Cyclops
Sylvania "A"	6/24/64	5/15/64	5/15/64	9/30/64	3/1/65	---[3]	---[3]	Sylvania

1. Sheet material produced by Fansteel under Contract NOw-63-0231-c and furnished to this program as transferred government owned material.
2. Second procurement action for this material.
3. Not included in program.
4. T-111 order split between three suppliers.
5. Converted at Westinghouse Astronuclear Laboratory.

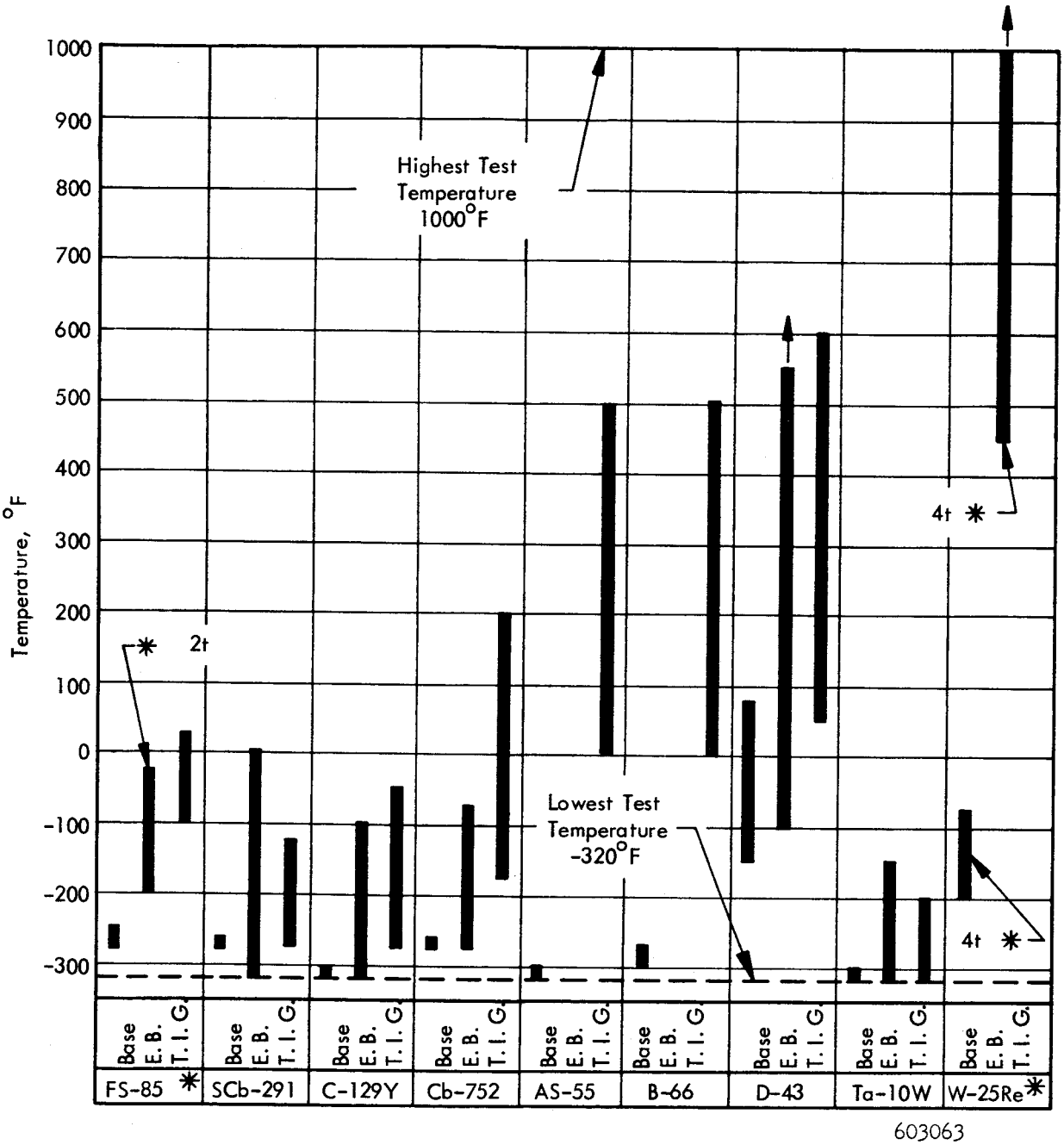

* — All bends 1t radius except FS-85 E. B. welds which are 2t radius and all W-25Re tests which are 4t radius.

FIGURE 1 - Summary of Current Bend Test Results for Butt Welds in 0.035 Inch Sheet.

Techniques were developed for gold-nickel brazing of platinum-platinum rhodium thermocouples into the high vacuum annealing furnace feedthroughs. An inert gas cover protects the joint while brazing is done by induction heating.

The TIG weld preheat fixture designed for use in welding W-25Re, unalloyed tungsten, and Sylvania "A" and was checked out satisfactorily at 450°F.

III. TECHNICAL PROGRAM

A. ALLOY PROCUREMENT

The procurement status of the alloys included in this program is shown in Table 2. During this period AS-55 and T-111 sheet were delivered. The as-received microstructure of AS-55 is shown in Figure 2. A summary of actual chemical composition for the as-received alloys is given in Table 3, while hardness and grain size values are given in Table 4. The check chemistry of AS-55 indicates excessively high oxygen. Other sections of this sheet are being rechecked to ascertain if the condition is general or local. The base metal bend test results for AS-55 are shown in Figure 3.

B. WELDING EVALUATIONS

1. TIG Welding

Sheet welding was completed for nine alloys for the parameter optimization phase and bend testing was completed for seven of these. Bend test results for TIG welds in these alloys are given in Figures 4 through 9, and 12 through 19. Weld parameters are listed in corresponding tables. TIG welding procedures and equipment were described in detail in previous quarterly reports in this program.[1]

A complete interpretation of these tests must be deferred until supplementary test data is generated through post weld anneals and tensile tests. A tentative weldability analysis based on the bend test results included in this report and upon observations made in the examination of the actual individual bend tested specimens is given below. Each specimen was examined for type, degree, and location of cracks. A cursory examination of weld bend transition temperatures for all alloys as a function of monitored oxygen and moisture levels failed to reveal that any relationship exists. Hence, the alloys are either insensitive to contaminants at these levels, the welding process itself has too much variability, or the meter accuracy is inadequate over the range evaluated.

The following observations were made in evaluating the bend test results for the sheet TIG welds in the various alloys:

B-66 (See Pages 16-18 for test data) - The longitudinal bend transition temperature was reduced from 200°F to 0°F by increasing the weld speed from 7.5 to 30 ipm. At and above 30 ipm, however, B-66 exhibited a tendency toward hot tearing and possibly micro-cracking during welding resulting in a sharp increase in transition temperature. The transverse bend transition temperature did not display a similar decrease with increased welding speed remaining roughly at 150°F. The frequency of cracking in weld and heat affected zone of bend specimens was about the same. These cracks were sometimes arrested in the base metal, but almost

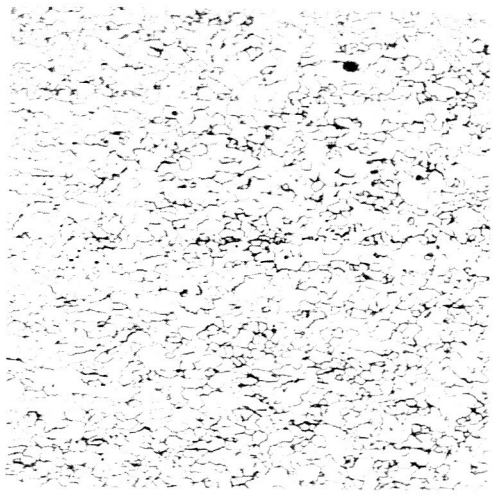

100X 6856

.035 Sheet

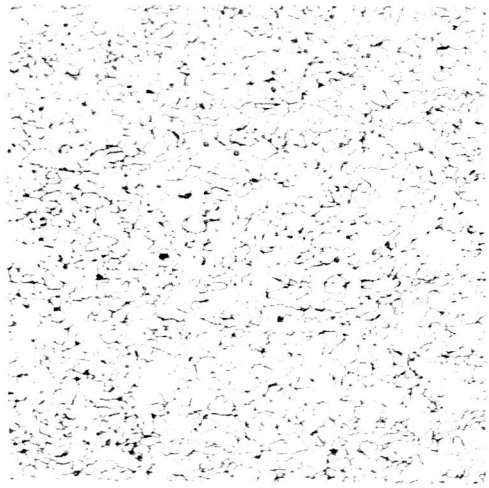

100X 6857

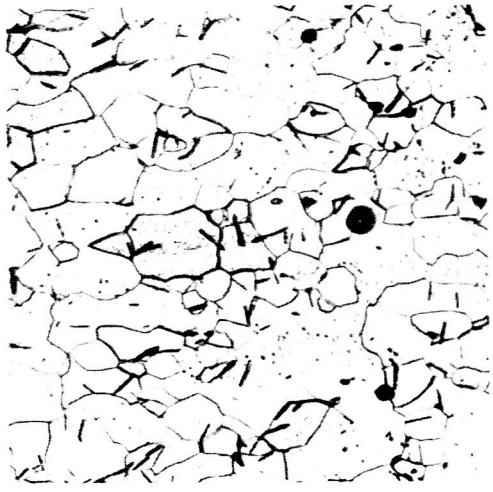

400X 6856

Longitudinal

.035 Sheet

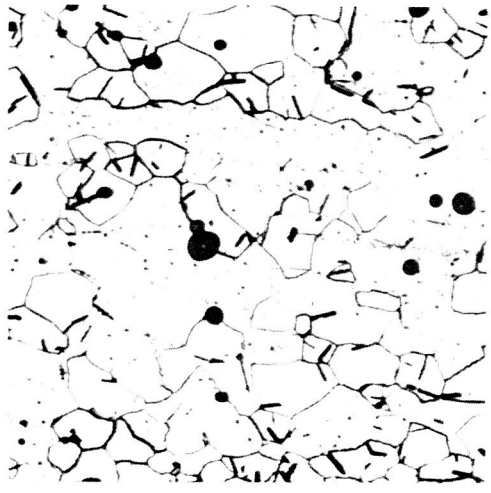

400X 6857

Transverse

FIGURE 2 - Microstructures of As-Received AS-55 Alloy Sheet (HNO_3-$NH_4F \cdot HF$ Etch)

TABLE 3 - Chemistry of As-Received Material

Alloy	Form	Heat	Certified Analysis (Avg.) w/o Zr	Hf	Mo	V	Y	Re	W	Ta	Cb	ppm C	O	N	Check Chemistry ppm C	O_2	N_2
AS-55	Sheet	430-7	1.07				0.02-0.3		4.74		Bal.	306	190-600	155	440	750	200
B-66	Plate	DX-609	1.00		5.17	4.89					Bal.	95	110	63	37	120	70
	Sheet	DX-609	1.00		5.17	4.89					Bal.	95	110	63	44	150	30
	Wire	DX-569	1.10		5.23	5.61					Bal.	17	70	64	130	140	90
		DX-603	0.92		4.55	4.85					Bal.	40	82	75	130	190	60
C-129Y	Plate	6.6-57033		10.25					10.8		Bal.	65	160	15	58	200	30
		610-57204		10.10					10.85		Bal.	80	50	58			
	Sheet	46-70617		9.5			0.105		9.8	0.135	Bal.	85	105	50	36	102	60
	Wire	6.6-57033		10.25					10.8		Bal.	65	160	15	52	120	50
Cb-752	Plate	52165	2.70						9.8		Bal.	50	76	10	16	84	70
	Sheet	52208	2.90						9.9		Bal.	40	143	102	21	180	80
	Wire	52183	2.90						9.6		Bal.	30	60	120	51	120	90
D-43	Plate	43-398-13	0.97						10.3		Bal.	835	63	32	930	64	20
	Sheet	43-398-13	1.00						9.9		Bal.	1046	200	32	1100	180	10
	Wire	43-372-1	0.88						9.7		Bal.	810	52	33		85	60
FS-85	Plate	85D-740	0.94						10.6	28.1	Bal.	20	90	60			
	Sheet	85D-739	0.95						10.43	27.61	Bal.	40	40	52	12	98	50
	Wire	85D-695	0.97						10.2	28.0	Bal.	20	40	30	34	73	40
SCb-291	Plate	2255							10.0	9.83	Bal.	20	110	40	22	101	20
	Sheet	1991							9.9	9.6	Bal.	12	65	76	17	110	50
	Wire	1825							10.1	9.2	Bal.	10	67	70	12	130	50
Ta-10W	Plate	60B-758							9.90	Bal.		50	40	20	5	10	10
	Sheet	60B-758							9.90	Bal.		50	40	20	12	66	100
	Wire	60B-609															
T-111	Plate	2691		1.7					7.05	Bal.		18.5	10	26	27	34	10
	Sheet	6-65042-Ta		2.0					8.8	Bal.		80	50	35			
	Wire	DX-571		2.01					8.12	Bal.		10	20	10	17	23	20
W-Re	Sheet	3.5-75002						25.6	Bal.			40	50	35	8	8	10
W	Sheet	KC-1350							Bal.						6	10	10
		KC-1353							Bal.						9	15	10

TABLE 4 - Hardness and Grain Size of As-Received Material

Alloy	Form	Hardness DPH	ASTM Grain Size
AS-55	Sheet	148	9
B-66	Plate	225	6
	Sheet	219	10
C-129Y	Plate	218	
	Sheet	185	10
Cb-752	Plate	204	8
	Sheet	205	8-9
D-43	Plate	202	
	Sheet	220	5
FS-85	Plate	205	7
	Sheet	190	8
SCb-291	Plate	160	6
	Sheet	175	6
Ta-10W	Plate	197	8
	Sheet	221	6-7
T-111	Plate	223	6-7
	Sheet	221	9
W-25Re	Sheet	526	*
		492	
W	Sheet	517	*

* Stress Relieved, Not Recrystallized

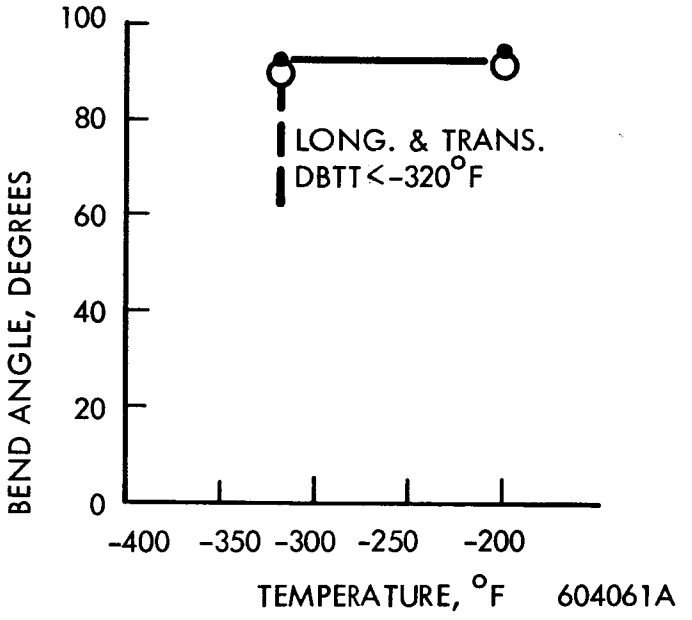

FIGURE 3 - AS-55 Base Metal Bend Test Results.
1t Bend Radius

as frequently propagated across the entire specimen. No definite clamp spacing effect was observed. Larger welds in the 15 ipm group had better longitudinal bend ductility possibly resulting from crowding of the clamp by the weld and consequent reduction in the size of the heat affected zone. These results indicate that embrittlement of B-66 occurs in the heat affected zone as well as in the weld.

C-129Y (See Pages 19-21 for test data) - Weld parameter variations did not result in demonstrating that any consistent improvement in weld ductility could be obtained. Weld transition temperatures were consistently low (-50°F to -275°F). The beneficial effect of yttrium is apparently instrumental in providing the improved ductility in welds of this alloy. The most probable mechanisms for accomplishing this are an effective reduction in matrix oxygen level by preferential combination with the yttrium, purification of base metal during original melting and during welding by slagging of the yttrium oxide, and base and weld metal grain refinement resulting from the presence of the highly stable oxide. Failures in the transverse tests occurred almost entirely in the weld or at the weld interface and generally at lower temperatures than in longitudinal tests. Longitudinal specimens generally failed across the entire specimen demonstrating that cracks initiated in the weld are not arrested in the base metal.

Cb-752 (See Pages 22-24 for test data) - A definite tendency is exhibited in the transverse weld bend test for the weld metal ductility to improve with welding speed. Longitudinal tests show no such definite trend thereby demonstrating that heat affected zone embrittlement is essentially unaffected over the range of selected welding conditions. Transverse fractures all occurred in the weld or heat affected zone. Longitudinal fractures were almost always across the entire specimen demonstrating the inability of the base metal of this alloy to arrest cracks at temperatures below the weld metal transition temperature.

D-43 (See Pages 28-30 for test data) - No definite effect of weld parameter variations were noted. Changes in weld size, freezing rate, and cooling rate resulted in no definite trend of improvement of the bend ductile-brittle transition temperature. Bend behavior of this alloy was peculiar since a typical transition curve did not develop, rather, overstraining and failure occurred near the 90° target bend over an extended temperature range. Obviously, for D-43 the bend test has defined a limitation for total strain as well as a ductile-to-brittle transition temperature. The intentional carbon addition in this alloy results in precipitation of a carbide phase(s) the morphology of which strongly influences alloy ductility. In this respect lot to lot variability in ductility would result from variation of process and welding schedules in production and fabrication and perhaps also from the relative variation of heat to heat carbon concentrations. Examination of the fractured specimens showed that loss of ductility was most pronounced in the weld but that fractures frequently

extended through and were not arrested in the base metal .

FS-85 (See Pages 31-33 for test data) - A slight improvement in weld transition temperatures occurred by minimizing the weld size in this alloy. Weld speed or clamp spacing appear to have little effect. Weld behavior was very consistent providing bend transitions within 75°F of -25°F for all welding conditions. All cracking was associated with the weld and heat affected zone. A definite tendency for cracks to propagate along the weld interface was noted.

SCb-291 (See Pages 34-36 for test data) - The weld bend transition temperature of SCb-291 is very nearly that of the base metal for all weld conditions. The equivalent ductility of base and weld metal is demonstrated by failure of the base metal to arrest cracks in longitudinal bends, and in the tendency of base metal to fail as frequently in transverse tests as does the weld metal. This is the only alloy in which the base metal failures were noted indicating, from a practical standpoint, that solid solution strengthening has been accomplished in this alloy system with a minimum impairment of weld ductility.

Ta-10W (See Pages 37-39 for test data) - Weld bend transition temperatures for this alloy were all in the range of -200°F to less than -320°F. Failures always occurred in the weld, generally as one or two very small tears. Variation of weld parameters failed to produce any pronounced trends.

2. Electron Beam Sheet Welding

A complete set of welds were produced for the D-43 and W-25Re alloys. The welds were bend tested and the results are presented in Figures 10, 11, and 21 to 24. The bend transition temperatures indicated are, as described in the previous quarterly report, those at which a 90° to 105° bend was obtained without cracking on the tension side of the specimen.

D-43 (See Pages 25-27 for test data) - Slower weld speeds and wide clamp spacing produced welds with the lowest bend transition temperatures. An examination of the transverse bend specimen revealed most of the strain and crack initiation occurred in the heat affected zone rather than in the unyielding weld metal. Longitudinal bend tests, which equally strain the entire specimen, initiated cracks in the weld metal, indicating the weld metal to be the least ductile area.

Bend transition temperatures varied from -100°F to more than 550°F, but considering only the welds with a good physical appearance (a few combinations of deflection and/or weld speed produced a deep ripple pattern in the weld), the range was reduced to -100°F to 200°F for the longitudinal bend test.

W-25Re (See Pages 40-45 for test data) - Some unexpected problems, both in material preparation and in welding, were encountered in the electron beam weld

evaluation of W-25Re alloy. Butt weld specimens of 0.035 inch sheet are normally prepared by shearing, but this operation caused edge cracking, possibly delaminations, in the sheared edge of W-25Re. In an effort to eliminate this condition, which could adversely affect the bend ductility, warm shearing at 600°F and abrasive cut-off wheel preparation were investigated. Warm shearing reduced the observed edge cracking considerably and abrasive cut-off wheel preparation was a further improvement, but neither method was completely satisfactory. Since abrasive cut-off wheel preparation is a tedious and expensive operation in preparing 6 inch long by 1/2 inch wide specimens, additional W-25Re butt weld specimens are being prepared for evaluation by electro-discharge machining (EDM) to be followed by edge grinding and pickling prior to welding.

Initial butt welding of sheet specimens by the electron beam process produced severe cambering and seam spreading in front of the weld. This resulted in immediate burn-through of the finely focused electron beam. The problem was solved by increasing the size of the electron beam tack welds made at either end of the butt seam prior to the single pass weld. The previously welded columbium base and tantalum base alloys all demonstrated the opposite tendency; that of tightly closing the butt joint ahead of the weld.

Initial bend tests were conducted with the 1t radius bend test punch used on the previously tested alloys, but an immediate change was made to a 4t punch radius when a ductile 90° bend could not be made within the 1000°F temperature limit of the bend test apparatus. All the W-25Re bend test data were obtained using a 4t punch radius except weld number 1 as indicated in Figure 21.

Bend transition temperatures were higher than anticipated, especially transverse bends wherein only one welding condition developed a transverse ductile-to-brittle transition temperature (600°F) within the range of the testing apparatus. All other welding conditions produced failures, though some were minute cracks, at the highest bend temperature of 1000°F.

An examination of some aborted butt weld specimens which had fractured down the weld centerline soon after welding, showed extreme cambering, with the weld edge concave, indicating severe residual longitudinal tensile stresses in the weld metal. On the basis that these high residual weld stresses could be contributing to apparent low bend ductility, a group of spare transverse bend specimens was vacuum stress relieved for one hour at 2560°F. Since the as-received material was stress relieved at the same temperature, no drastic morphological changes were anticipated in at least the base metal.

Following the stress relief additional transverse bend tests were made for nearly all the welding parameters and the results are compared in Figures 23 and 24. A significant improvement in bend ductility is shown, presumably caused

by a reduction in weld residual stresses. This additional data, with ductile 90° bends now in the range of our testing apparatus, should allow a more accurate selection of the best welding parameters.

W-25Re EB Weld Summary - Slow welds (15 ipm) and wide clamp spacing produced welds with the lowest ductile-to-brittle bend transition temperature.

Relating this to the stress-relief bend ductility improvements, the low speed, high heat input, and slowly cooled welds possibly provide a greater degree of pre-and post-weld heating, thus reducing the weld induced residual stresses.

In view of the disappointing electron beam welding results obtained, additional investigation appears to be warranted both to verify our present results, identify the basic causes for embrittlement, and to develop a more satisfactory welding process.

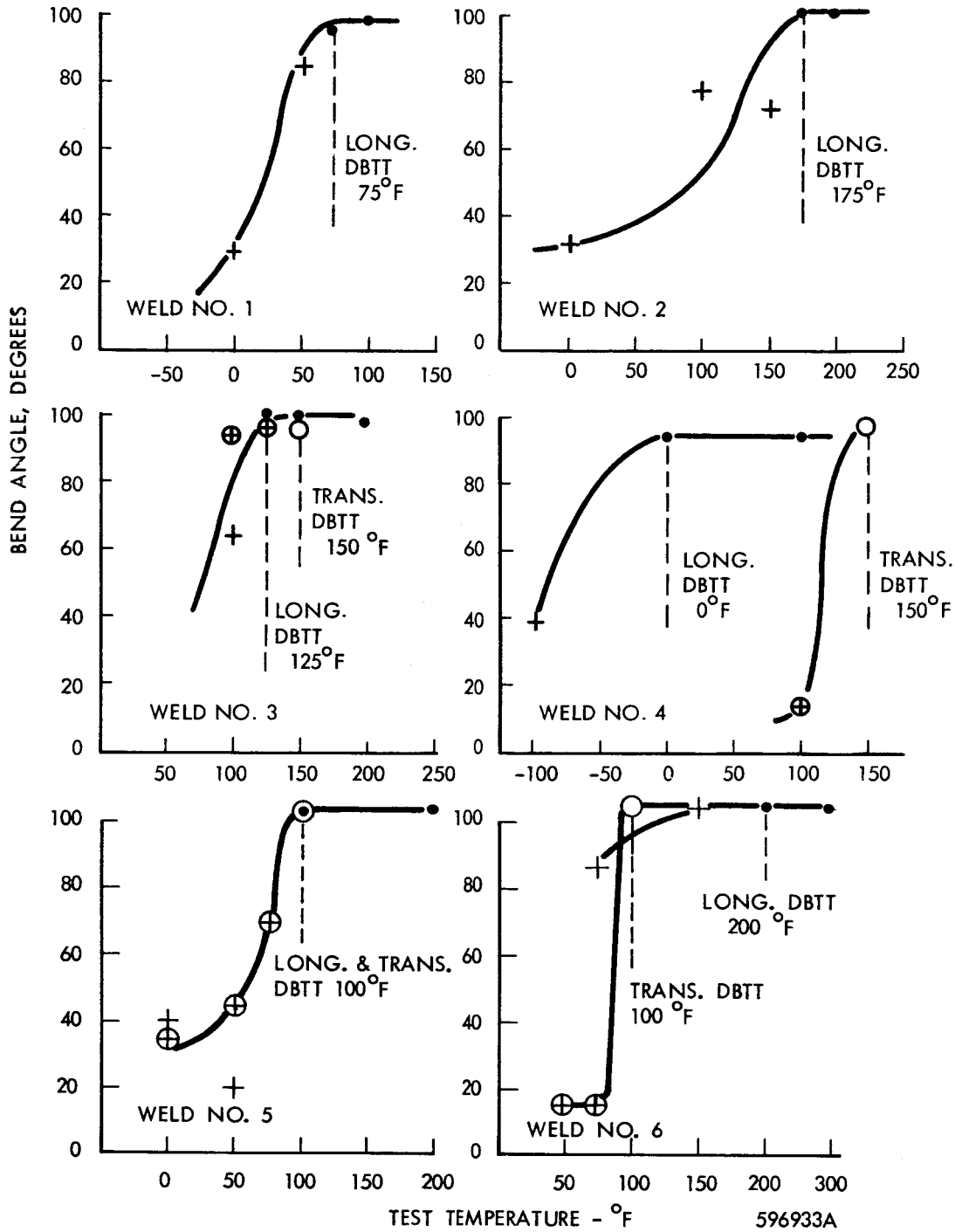

FIGURE 4 - B-66 TIG Weld Bend Test Results. 1t Bend Radius. For Weld Record See Table 5

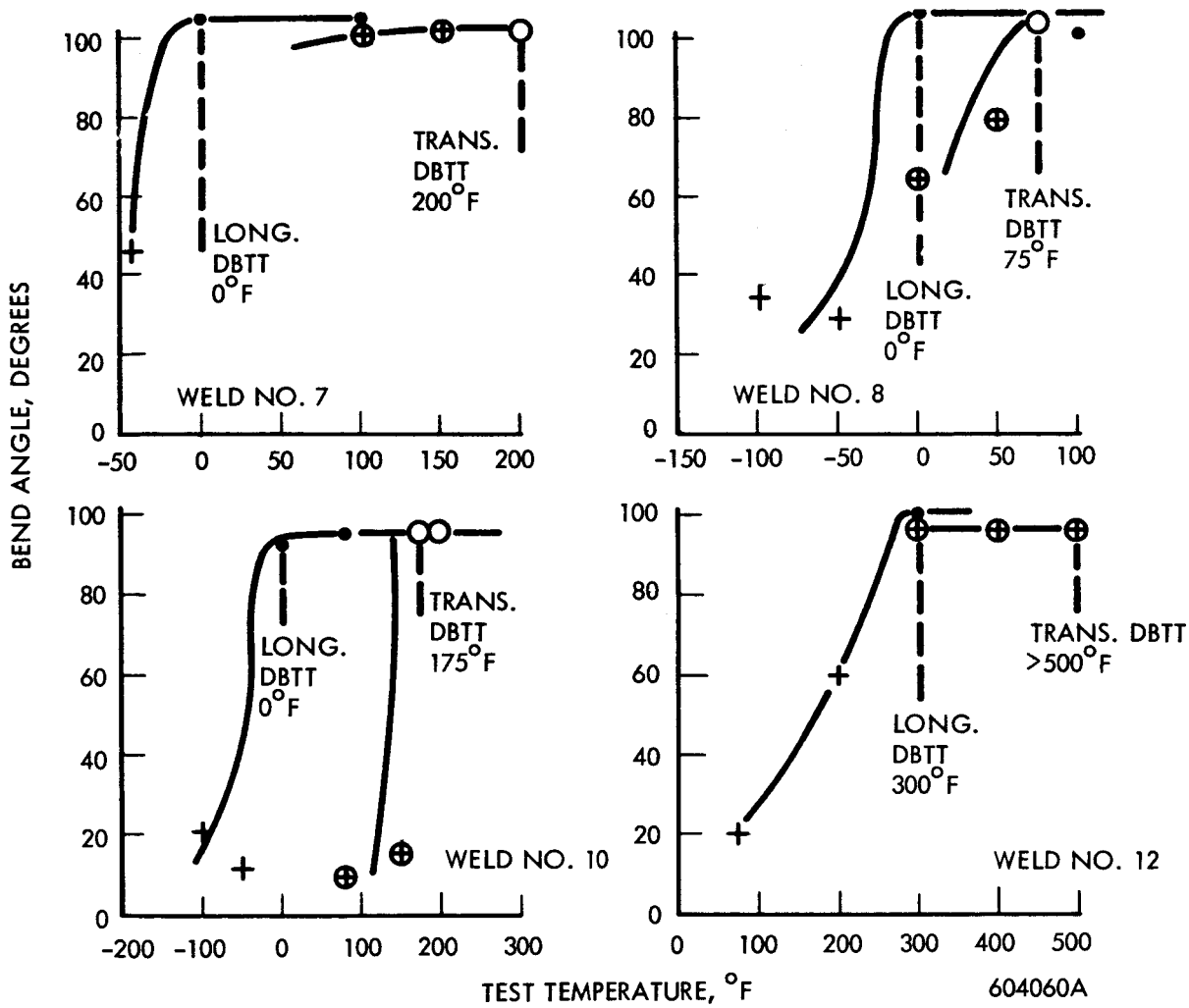

FIGURE 5 - B-66 TIG Weld Bend Test Results. 1t Bend Radius. For Weld Record See Table 5

TABLE 5 - B-66 Sheet. TIG Butt Weld Record

Weld No.	Clamp Spacing (inch)	Speed (ipm)	Current Amperes	Weld Width Top/Bottom (inch)	Q Joules/Inch	Atmosphere Monitor Readings			Comments	
						O_2(1) ppm	O_2(2) ppm	H_2O(3) ppm	Visual Inspection	Dye Check
1	3/8	15	50	0.11/0.07	3,400	--	3.5	2.3	Negative	Negative
2	3/8	15	70	0.13/0.08	4,750	--	4.5	0.5	Negative	Negative
3	1/4	15	80	0.135/0.110	5,420	5.0	5.4	0.05	1/2" Centerline Starting Crack	Positive
4	1/4	30	90	0.115/0.075	3,060	5.0	5.4	0.15	Edge Flash(4)	Negative
5	1/4	7.5	86	0.184/0.168	12,400	--	3.2	0.5	Starting Crack	Positive
6	3/8	7.5	60	0.136/0.100	8,380	1.0	3.5	0.35	Negative	Negative
7	1/4	15	113	0.200/0.196	8,140	0.7	2.5	0.1	Negative	Negative
8	3/8	15	86	0.190/0.180	6,020	0.3	2.4	0.1	Negative	Negative
9	1/4	30	170	0.231/0.228	6,460	2.0	2.4	0.05	Many Small Hot Tears	Positive
10	3/8	30	114	0.156/0.135	4,100	--	2.2	0.1	Negative	Negative
11	1/4	60	200	0.18/0.164	3,700	1.0	3.0	0.1	Many Small Hot Tears	Positive
12	1/4	60	165	0.138/0.090	3,050	1.0	2.0	0.2	Negative	Negative

(1) Westinghouse Oxygen Gage
(2) Lockwood & McLorie Oxygen Gage
(3) CEC Moisture Monitor
(4) Instantaneous Arcing to Weld Clamp Down

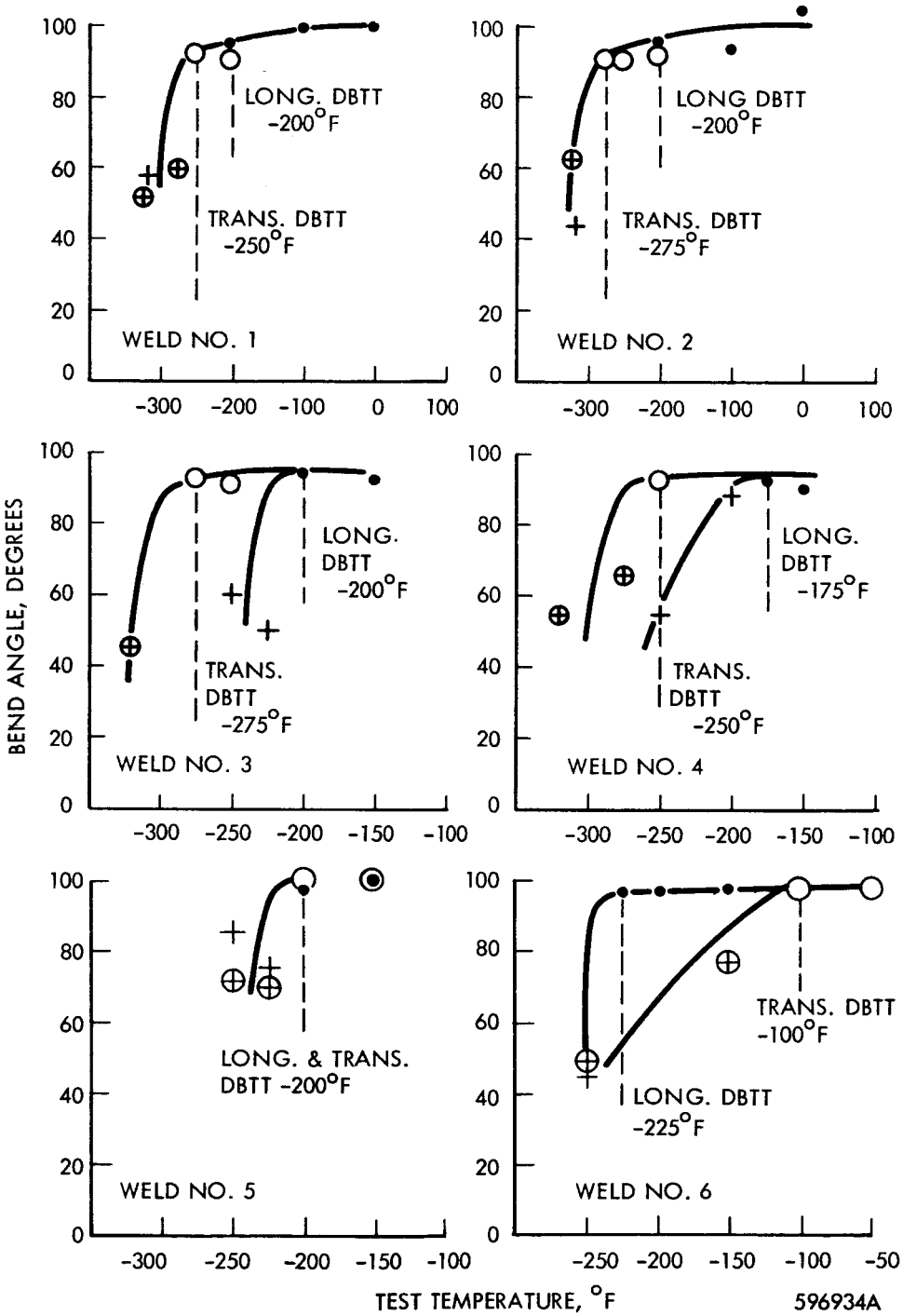

FIGURE 6 - C-129Y TIG Weld Bend Test Results. 1t Bend Radius. For Weld Record See Table 6.

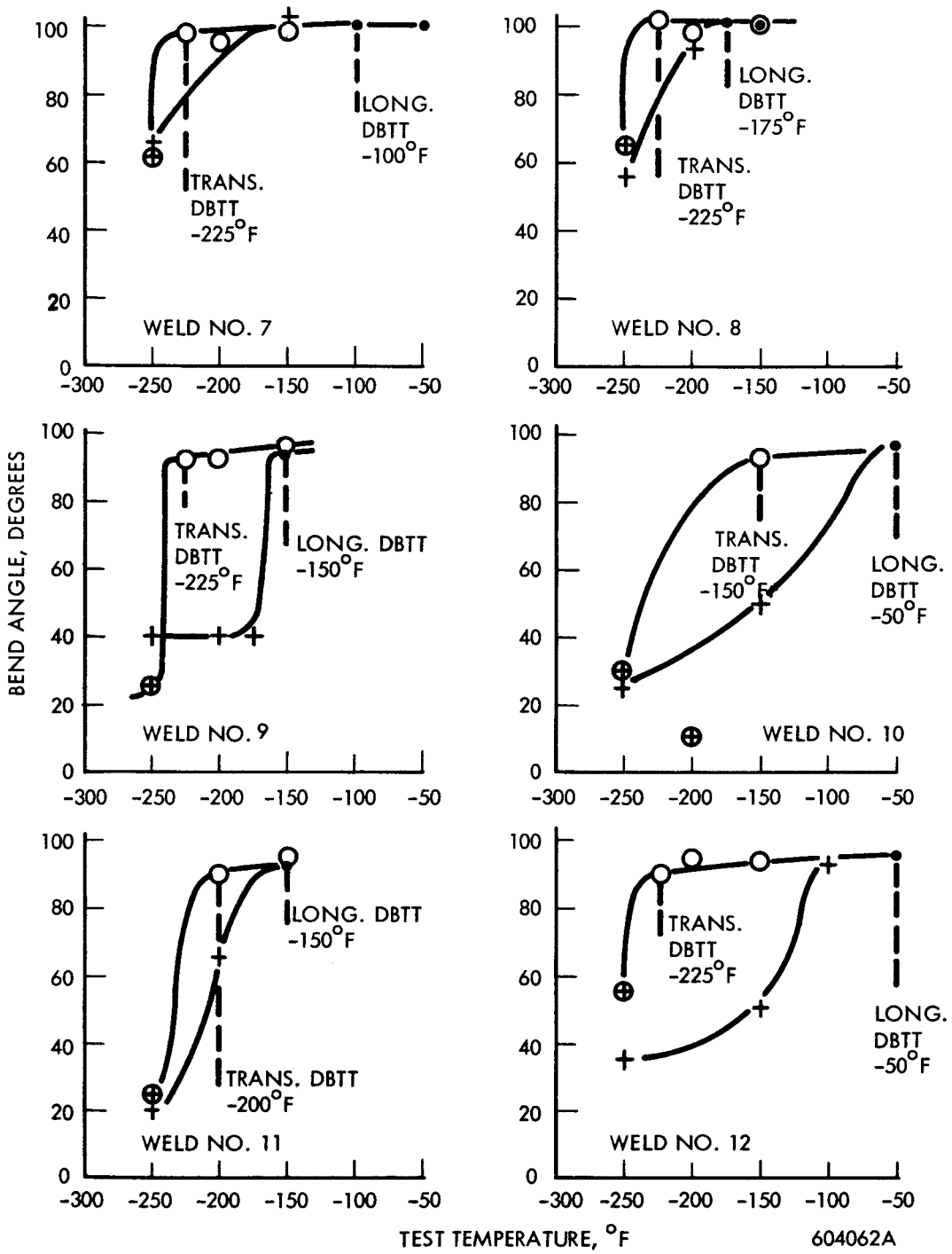

FIGURE 7 - C-129Y TIG Weld Bend Test Results. 1t Bend Radius. For Weld Record See Table 6

TABLE 6 - C-129Y Sheet. TIG Butt Weld Record

Weld No.	Clamp Spacing (inch)	Speed (ipm)	Current Amperes	Weld Width Top/Bottom (inch)	Q Joules/Inch	Atmosphere Monitor Readings			Comments	
						O_2(1) ppm	O_2(2) ppm	H_2O(3) ppm	Visual Inspection	Dye Check
1	3/8	15	70	0.150/0.10	4,750	3.5	--	0.7	Negative	Negative
2	3/8	30	110	0.18/0.13	3,730	3.5	--	0.9	Negative	Negative
3	1/4	15	80	0.15/0.11	5,430	4.0	4.7	2.0	Edge Flash(4)	Negative
4	1/4	30	102	0.145/0.115	3,460	4.5	4.8	2.1	Edge Flash(4)	Negative
5	1/4	7.5	74	0.160/0.116	10,950	1.5	3.3	0.8	Negative	Negative
6	1/4	7.5	93	0.180/0.150	13,750	4.0	3.6	2.9	Negative	Negative
7	3/8	7.5	62	0.159/0.132	8,680	1.8	3.9	1.7	Negative	Negative
8	3/8	15	95	0.219/0.204	7,030	2.0	4.2	2.0	Negative	Negative
9	1/4	30	150	0.180/0.165	5,560	0.5	2.1	0.3	Negative	Negative
10	3/8	60	170	0.150/0.135	3,140	1.0	2.3	0.3	Negative	Negative
11	3/8	60	145	0.120/0.075	2,680	--	1.8	2.8	Negative	Negative
12	1/4	60	150	0.120/0.075	2,780	1.5	3.5	1.0	Negative	Negative

(1) Westinghouse Oxygen Gage
(2) Lockwood & McLorie Oxygen Gage
(3) CEC Moisture Monitor
(4) Instantaneous Arcing to Weld Clamp Down

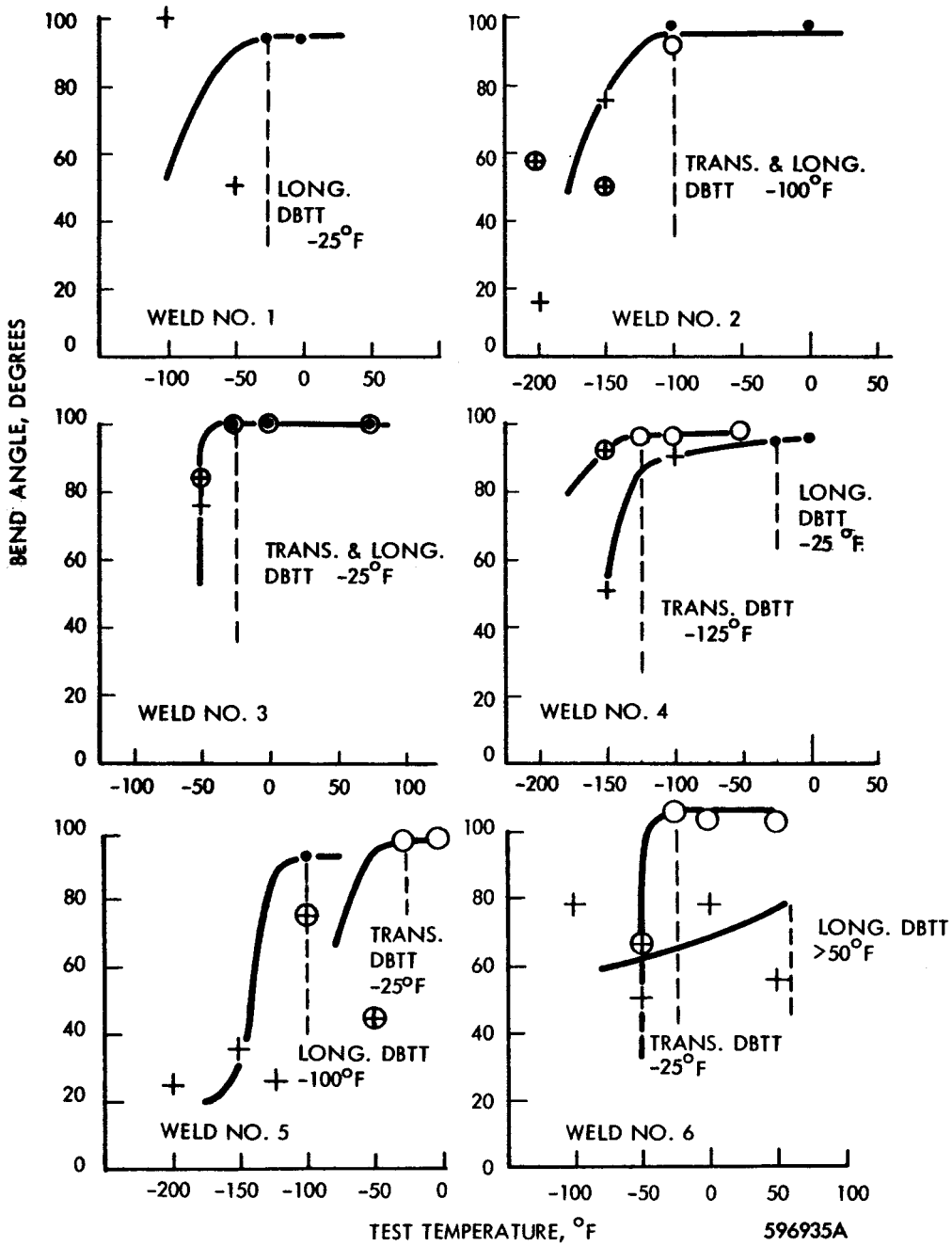

FIGURE 8 - Cb-752 TIG Weld Bend Test Results. 1t Bend Radius. For Weld Record See Table 7.

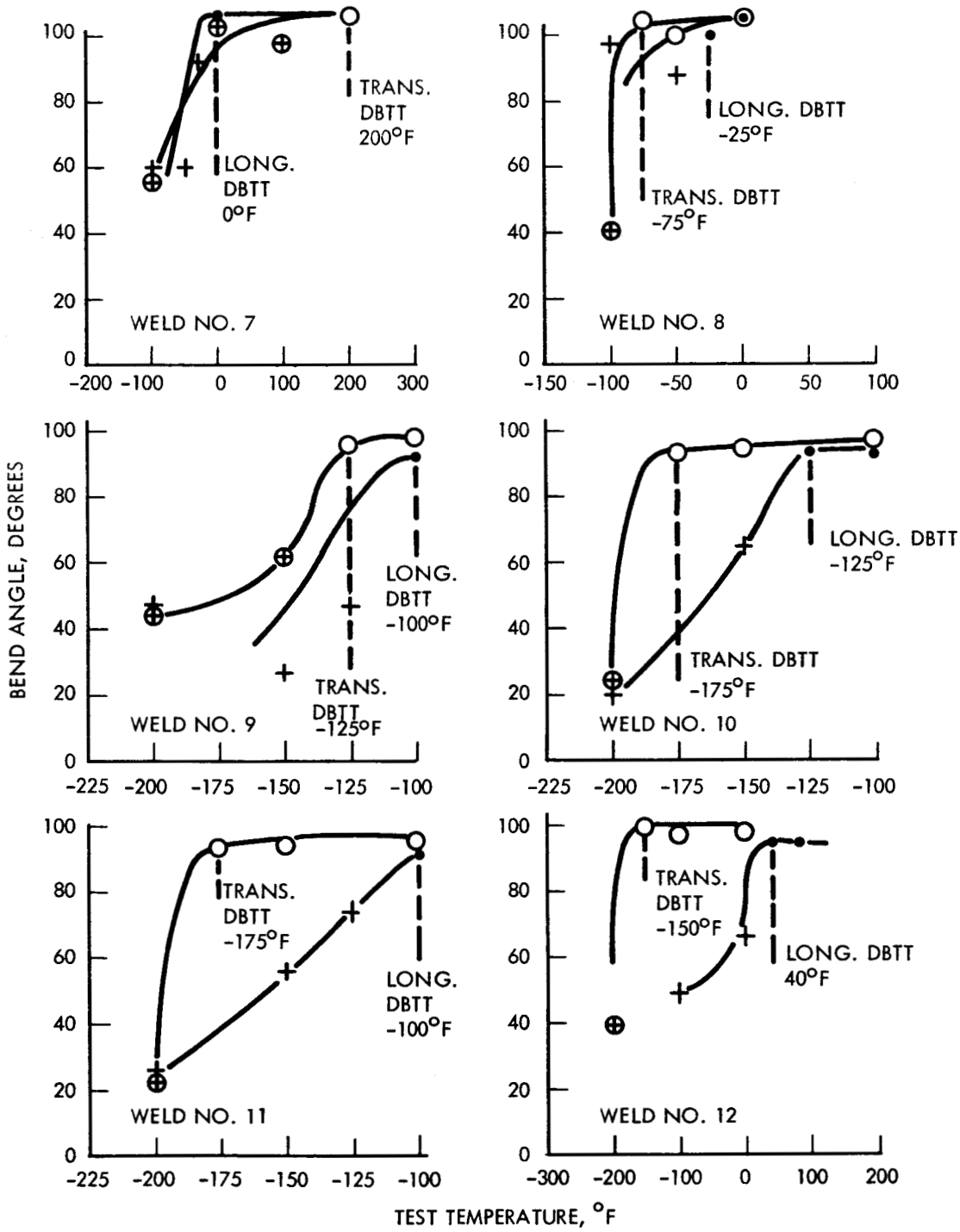

604057A

FIGURE 9 - Cb-752 TIG Weld Bend Test Results. 1t Bend Radius. For Weld Record See Table 7.

TABLE 7 - Cb-752 Sheet. TIG Butt Weld Record

Weld No.	Clamp Spacing (inch)	Speed (ipm)	Current Amperes	Weld Width Top/Bottom (inch)	Q Joules/Inch	Atmosphere Monitor Readings			Comments	
						O_2(1) ppm	O_2(2) ppm	H_2O(3) ppm	Visual Inspection	Dye Check
1	3/8	15	70	0.130/0.080	4,750	--	4.8	0.8	Negative	Negative
2	3/8	30	110	0.160/0.140	3,730	4.0	--	0.4	1/8" HAZ Crack	1/8" HAZ Crack
3	1/4	15	80	0.155/0.120	5,430	3.0	3.9	0.1	Edge Flash(4)	Negative
4	1/4	30	100	0.135/0.100	3,390	3.0	3.7	0.2	Edge Flash(4)	Negative
5	1/4	7.5	60	0.114/0.060	8,880	0.5	2.8	0.1	Negative	Negative
6	1/4	7.5	86	0.200/0.190	12,000	--	3.2	0.5	Negative	Negative
7	3/8	7.5	64	0.174/0.135	9,460	--	3.2	0.05	Negative	Negative
8	1/4	15	92	0.174/0.150	6,820	--	2.8	0.05	Negative	Negative
9	1/4	30	149	0.192/0.180	5,520	--	1.0	3.1	Negative	Negative
10	3/8	30	87	0.129/0.090	3,310	--	2.6	2.2	Negative	Negative
11	1/4	60	170	0.141/0.090	3,230	--	2.9	2.4	Negative	Negative
12	1/4	60	215	0.156/0.138	4,090	--	3.2	0.5	Negative	Negative

(1) Westinghouse Oxygen Gage
(2) Lockwood & McLorie Oxygen Gage
(3) CEC Moisture Monitor
(4) Instantaneous Arcing to Weld Clamp Down

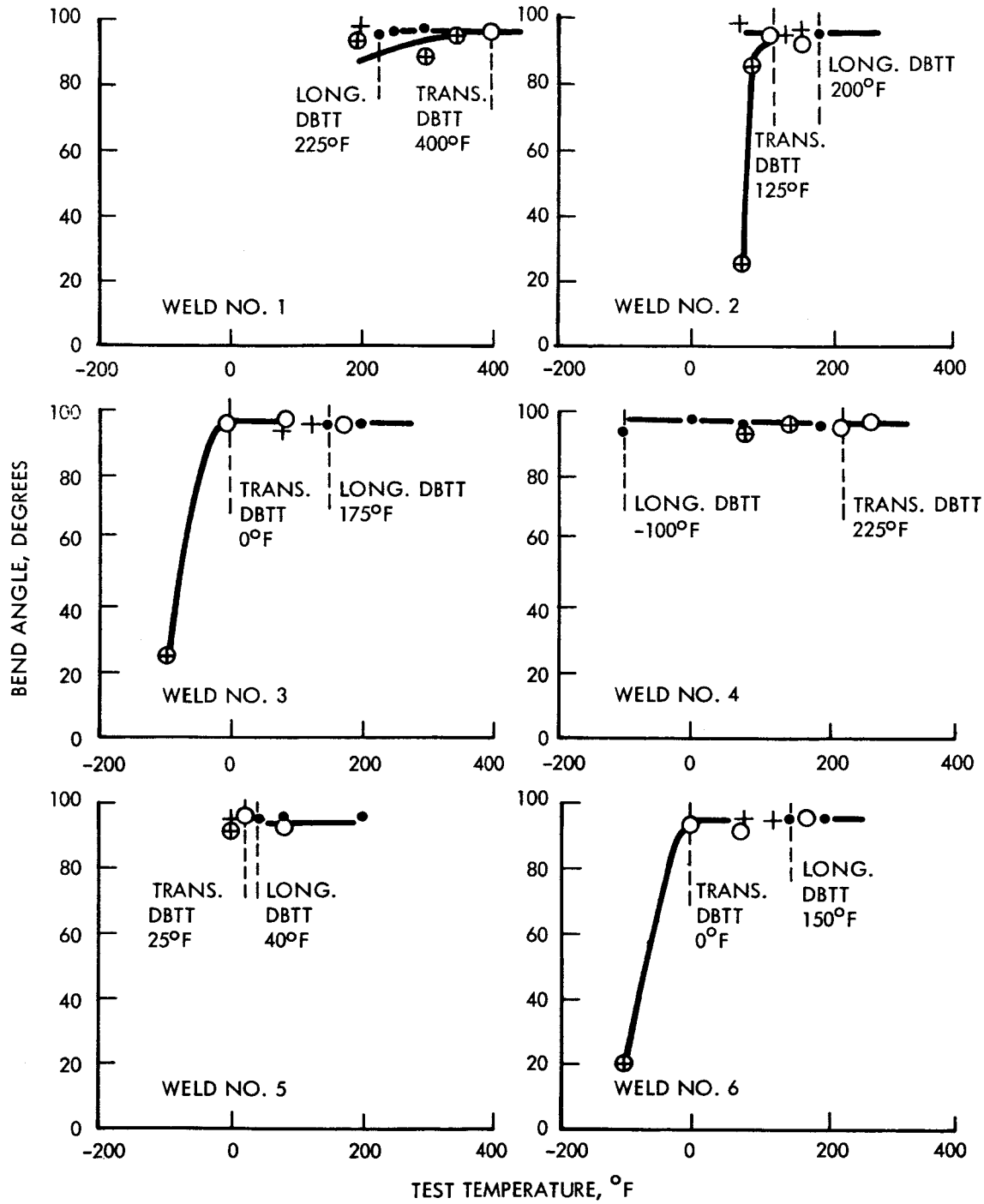

604059A

FIGURE 10 - D-43 EB Weld Bend Test Results. 1t Bend Radius. For Weld Record See Table 8.

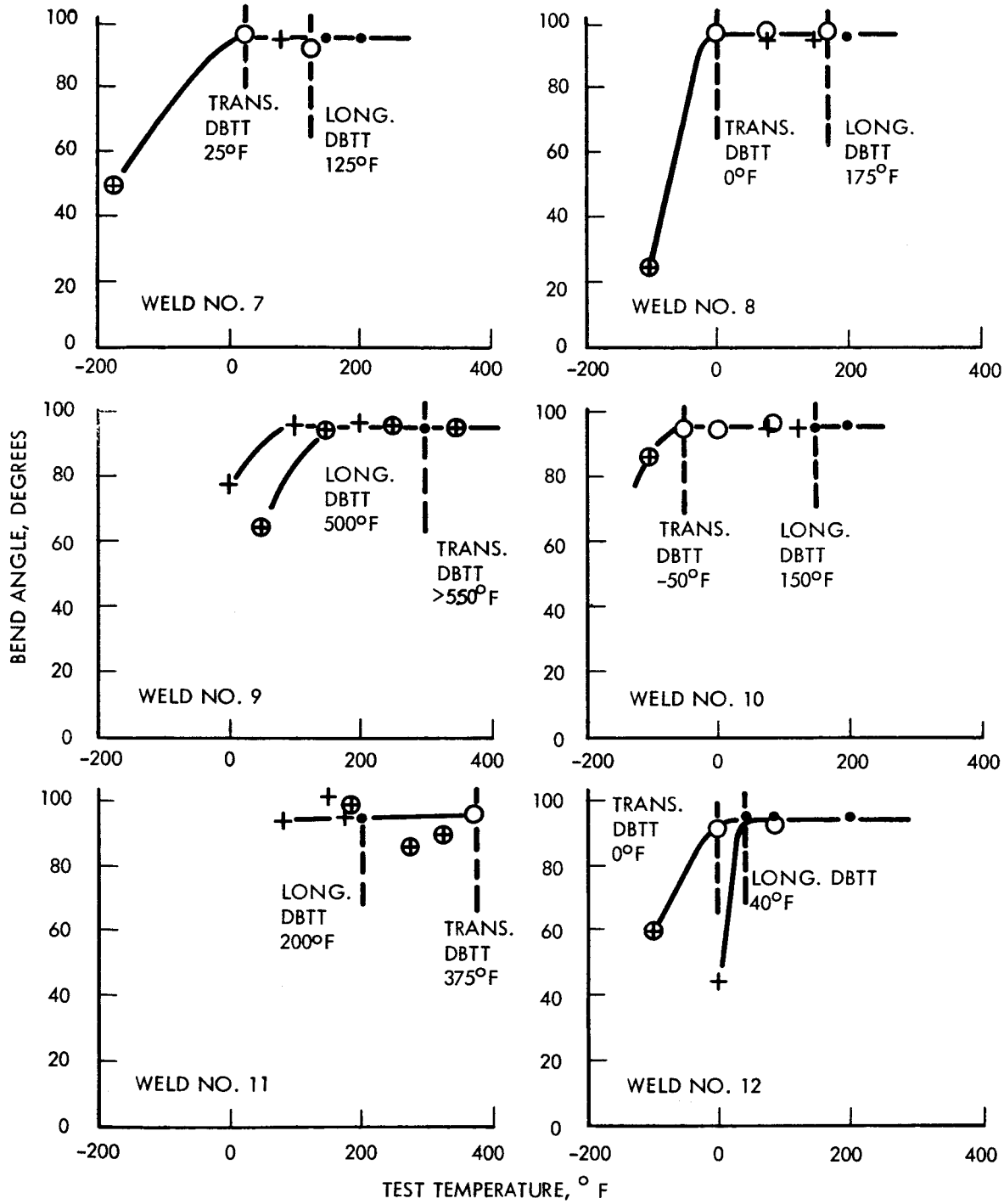

604058A

FIGURE 11 - D-43 EB Weld Bend Test Results. 1t Bend Radius. For Weld Record See Table 8.

TABLE 8 - Electron Beam Welding Parameters for D-43

Weld No.	Speed (ipm)	Deflection[1] (inches)	Current (ma)	Chill Spacing (inches)	Power[2] (watts)	Watt-Sec. per inch	Weld Bead Width (inches)		Vacuum Torr
							Top	Bottom	
1	50	zero	4.2	0.094	630	758	0.036	0.024	2.0×10^{-6}
2	100	L-0.050	6.0	0.094	900	540	0.034	0.029	2.0×10^{-6}
3	50	L-0.025	4.8	0.094	720	865	0.036	0.027	2.0×10^{-6}
4	15	L-0.050	3.3	0.250	496	1980	0.045	0.037	2.0×10^{-6}
5	50	L-0.050	4.4	0.250	660	793	0.040	0.027	2.0×10^{-6}
6	100	L-0.050	5.5	0.250	825	495	0.037	0.024	2.0×10^{-6}
7	50	L-0.050	4.8	0.094	722	868	0.040	0.027	2.0×10^{-6}
8	50	L-0.100	5.4	0.094	812	976	0.040	0.026	2.0×10^{-6}
9	15	zero	3.0	0.094	450	1800	0.039	0.029	2.0×10^{-6}
10	15	L-0.050	3.6	0.094	540	2160	0.044	0.027	2.0×10^{-6}
11	15	T-0.050	3.6	0.094	540	2160	0.060	0.050	2.0×10^{-6}
12	25	L-0.050	4.2	0.094	630	1510	0.040	0.035	3.0×10^{-6}

1. L. is longitudinal
   T. is transverse

2. All welds made at 150KV.

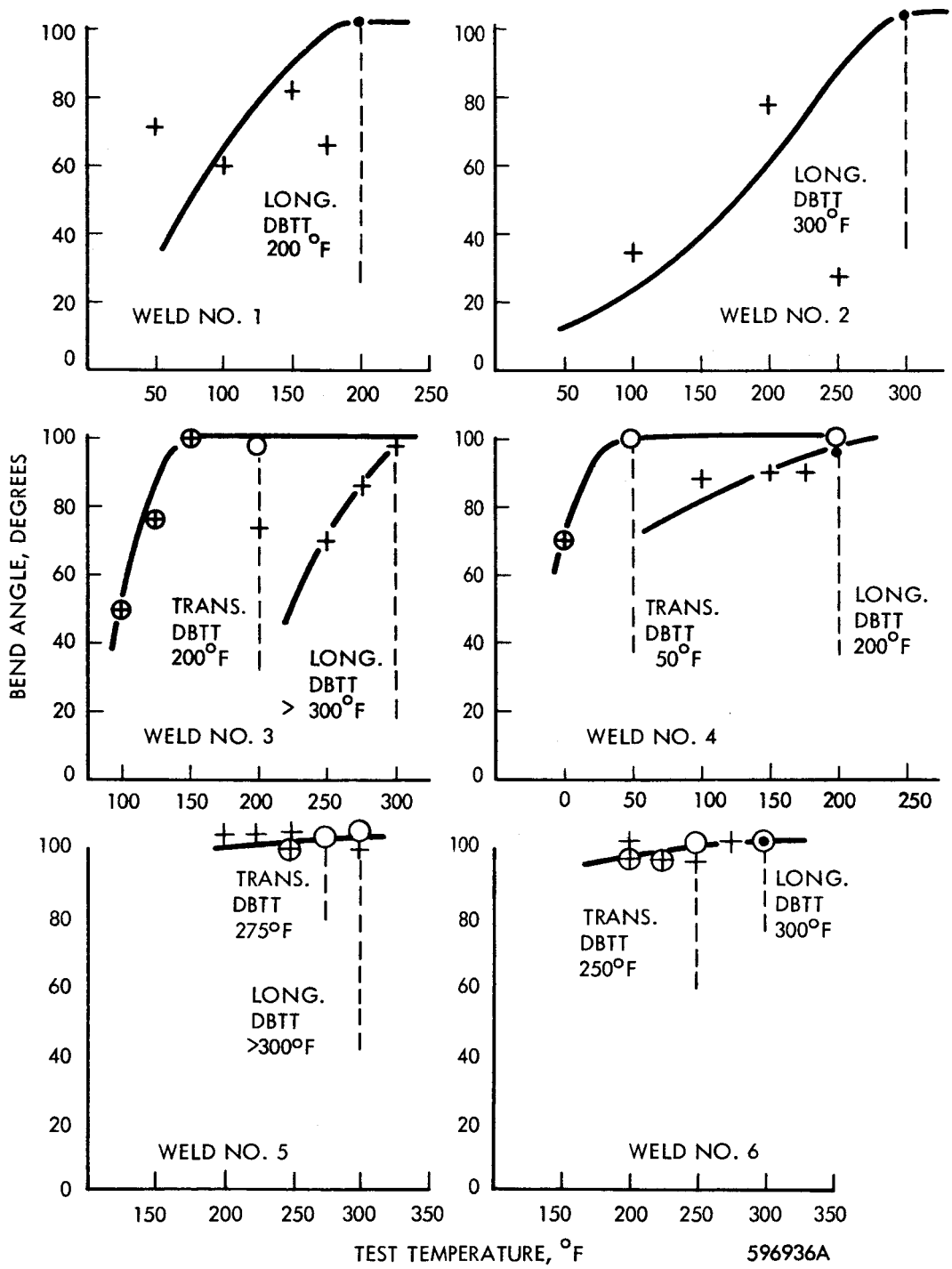

FIGURE 12 - D-43 TIG Weld Bend Test Results. 1t Bend Radius. For Weld Record See Table 9.

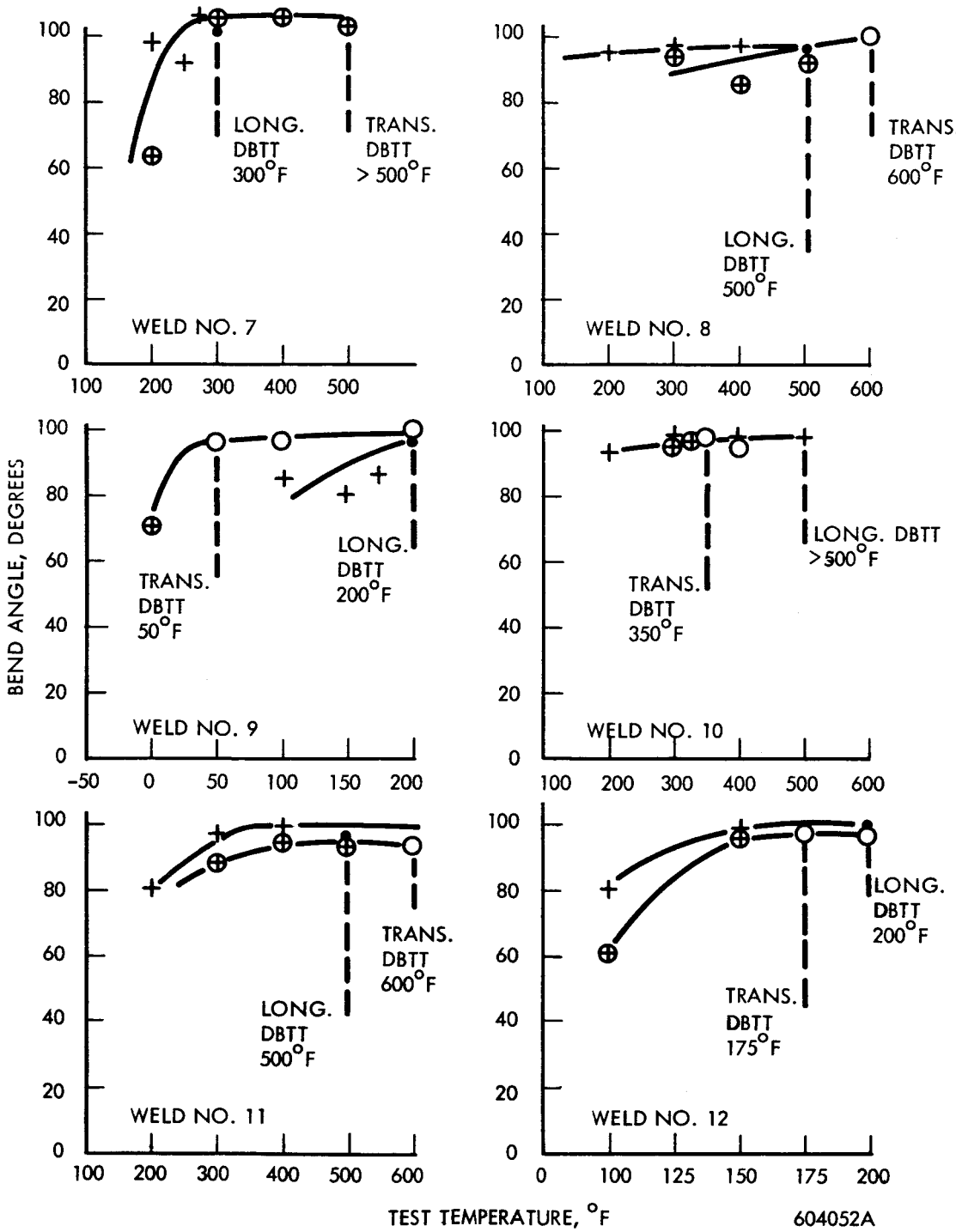

FIGURE 13 - D-43 TIG Weld Bend Test Results. 1t Bend Radius. For Weld Record See Table 9.

TABLE 9 - D-43 Sheet. TIG Butt Weld Record

Weld No.	Clamp Spacing (inch)	Speed (ipm)	Current Amperes	Weld Width Top/Bottom (inch)	Q Joules/Inch	Atmosphere Monitor Readings			Comments	
						O_2(1) ppm	O_2(2) ppm	H_2O(3) ppm	Visual Inspection	Dye Check
1	-3/8	15	60	0.10/0.02	4,080	--	4.3	0.17	Negative	Negative
2	3/4	15	80	0.18/0.18	5,420	--	4.3	0.40	Negative	Negative
3	1/4	15	75	0.14/0.12	5,100	5.0	5.5	0.20	Edge Flash(4)	Negative
4	1/4	30	100	0.135/0.09	3,390	6.0	5.9	0.40	Negative	Negative
5	1/4	7.5	65	0.120/0.09	9,340	3.5	4.4	2.2	Negative	Negative
6	1/4	7.5	82	0.190/0.190	11,800	4.0	4.6	2.4	Negative	Negative
7	1/4	15	122	0.240/0.240	9,020	0.5	2.4	0.15	Negative	Negative
8	1/4	30	135	0.165/0.150	5,000	--	2.0	0.5	Negative	Negative
9	3/8	30	114	0.159/0.144	4,550	0.5	2.2	0.30	Negative	Negative
10	3/8	30	72	0.099/0.024	2,590	0.5	2.1	0.40	Negative	Negative
11	3/8	60	155	0.129/0.075	2,865	0.5	2.7	0.30	Negative	Negative
12	1/4	60	215	0.180/0.165	4,090	2.0	3.2	0.10	Negative	Negative

(1) Westinghouse Oxygen Gage
(2) Lockwood & McLorie Oxygen Gage
(3) CEC Moisture Monitor
(4) Instantaneous Arcing to Weld Clamp Down

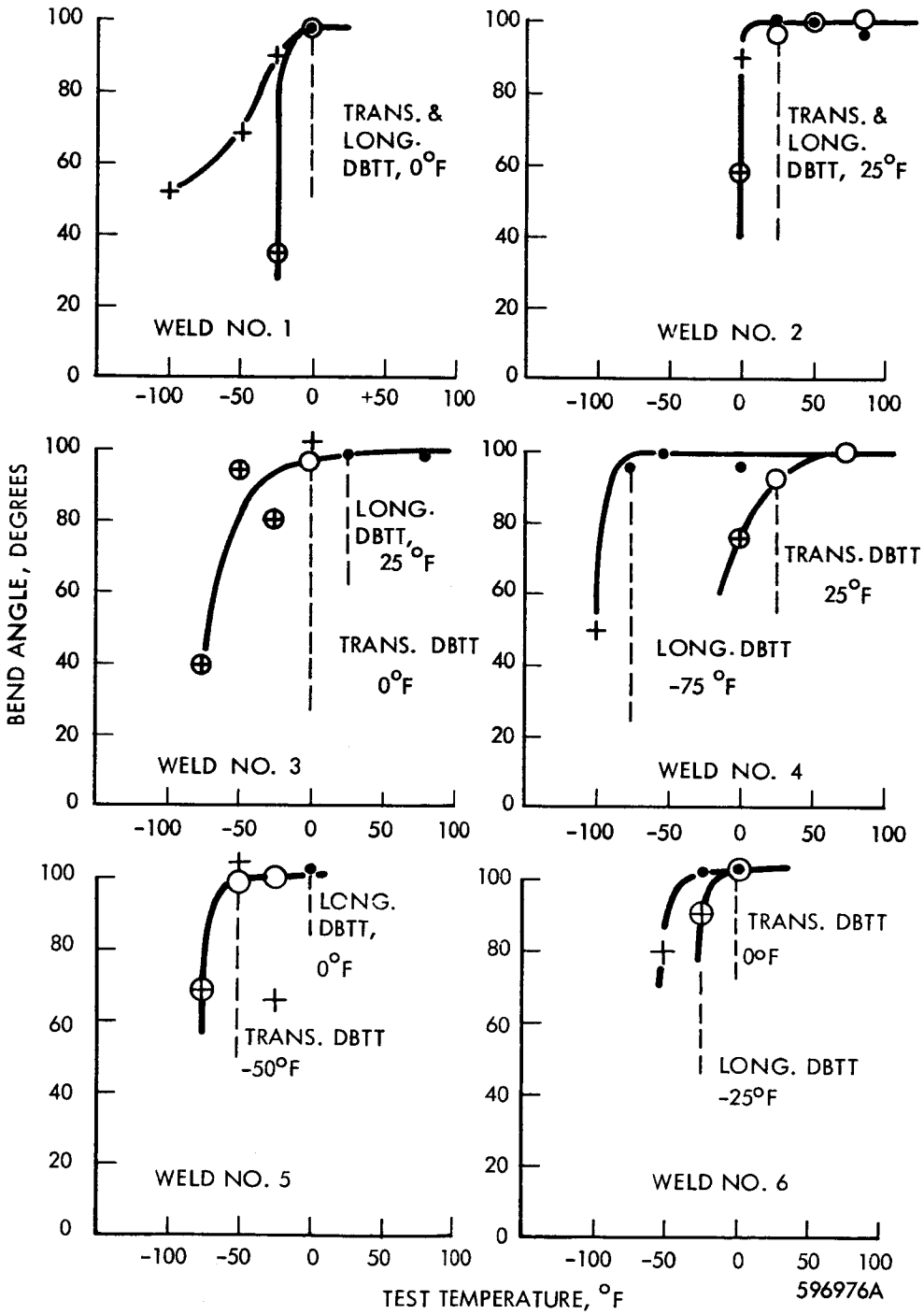

FIGURE 14 - FS-85 TIG Weld Bend Test Results. 1t Bend Radius. For Weld Record See Table 10.

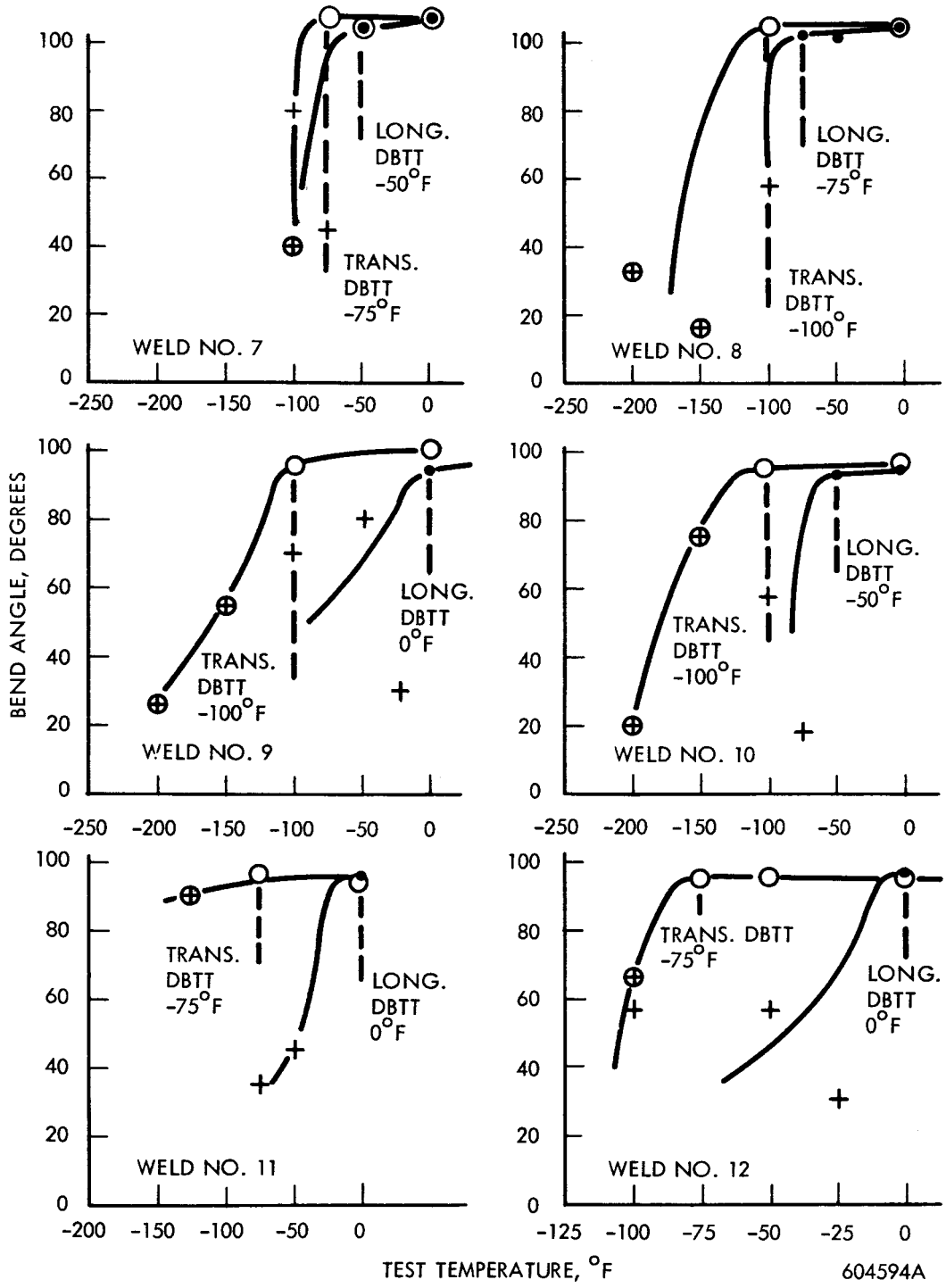

FIGURE 15 - FS-85 TIG Weld Bend Test Results. 1t Bend Radius. For Weld Record See Table 10.

TABLE 10 - FS-85 Sheet. TIG Butt Weld Record

Weld No.	Clamp Spacing (inch)	Speed (ipm)	Current Amperes	Weld Width Top/Bottom (inch)	Q Joules/Inch	Atmosphere Monitor Readings			Comments	
						O_2(1) ppm	O_2(2) ppm	H_2O(3) ppm	Visual Inspection	Dye Check
1	3/8	15	70	0.14/0.11	4,770	4.5	--	1.8	Negative	Negative
2	3/8	30	110	0.17/0.15	3,730	4.5	--	1.9	Negative	1/16" HAZ Crack
3	1/4	15	85	0.15/0.135	5,800	4.0	6.2	0.5	Edge Flash(4)	Negative
4	1/4	30	104	0.135/0.110	3,540	4.5	5.5	0.6	Edge Flash(4)	Negative
5	1/4	7.5	64	0.120/0.080	9,460	3.0	4.0	1.7	Negative	Negative
6	3/8	7.5	75	0.190/0.190	10,800	3.5	4.6	1.9	Negative	Negative
7	3/8	15	95	0.204/0.195	7,030	2.2	4.6	2.5	Negative	Negative
8	3/8	30	85	0.11/0.060	3,140	2.3	4.6	2.7	Negative	Negative
9	1/4	30	169	0.216/0.216	6,410	1.0	3.4	2.5	Negative	Negative
10	1/4	60	155	0.117/0.060	3,865	0.5	3.2	3.2	Negative	Negative
11	1/4	60	210	0.17/0.17	3,880	1.4	--	1.4	Negative	Negative
12	3/8	60	185	0.168/0.15	3,420	--	2.3	0.3	Negative	Negative

(1) Westinghouse Oxygen Gage
(2) Lockwood & McLorie Oxygen Gage
(3) CEC Moisture Monitor
(4) Instantaneous Arcing to Weld Clamp Down

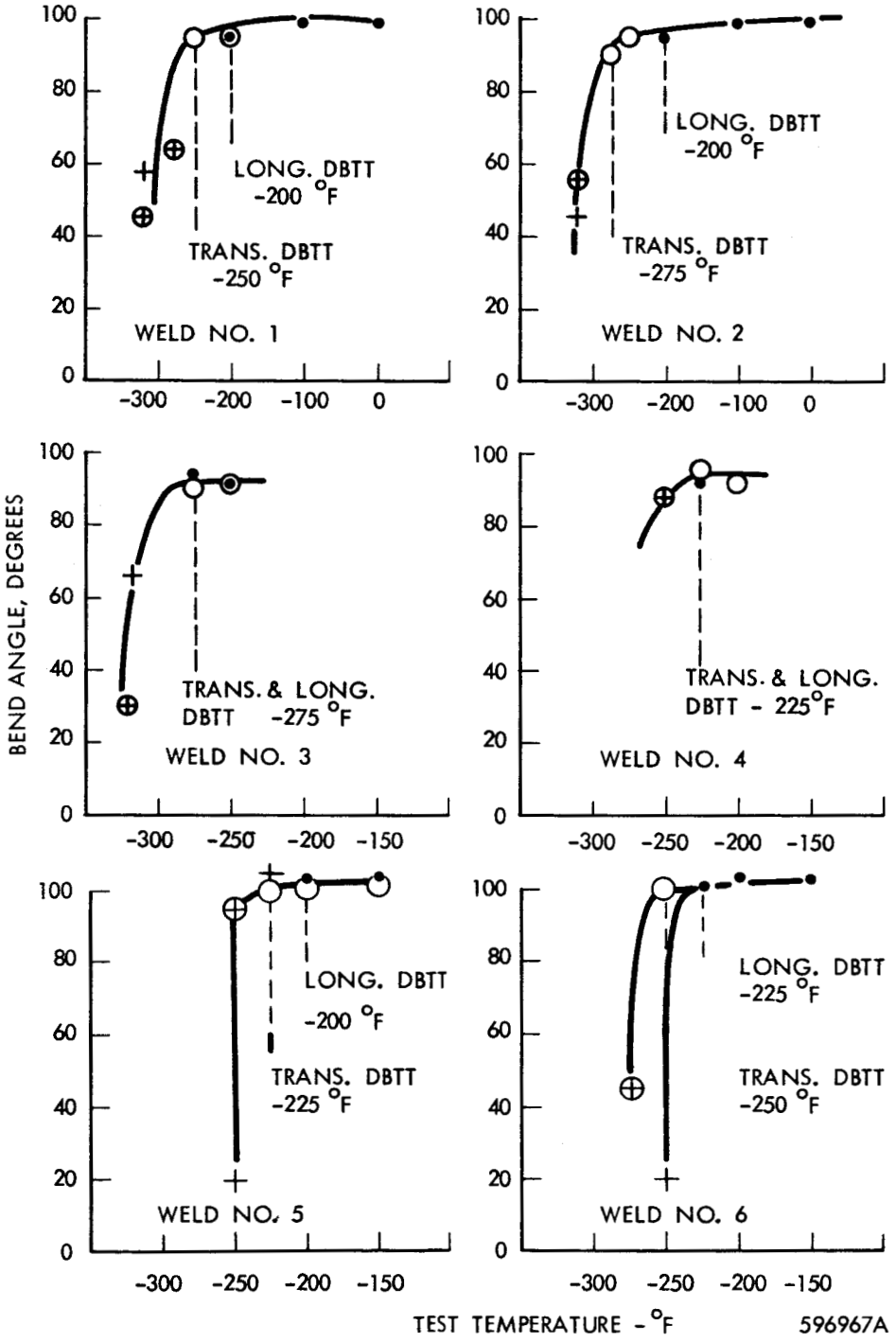

FIGURE 16 - SCb-291 TIG Weld Bend Test Results. 1t Bend Radius. For Weld Record See Table 11.

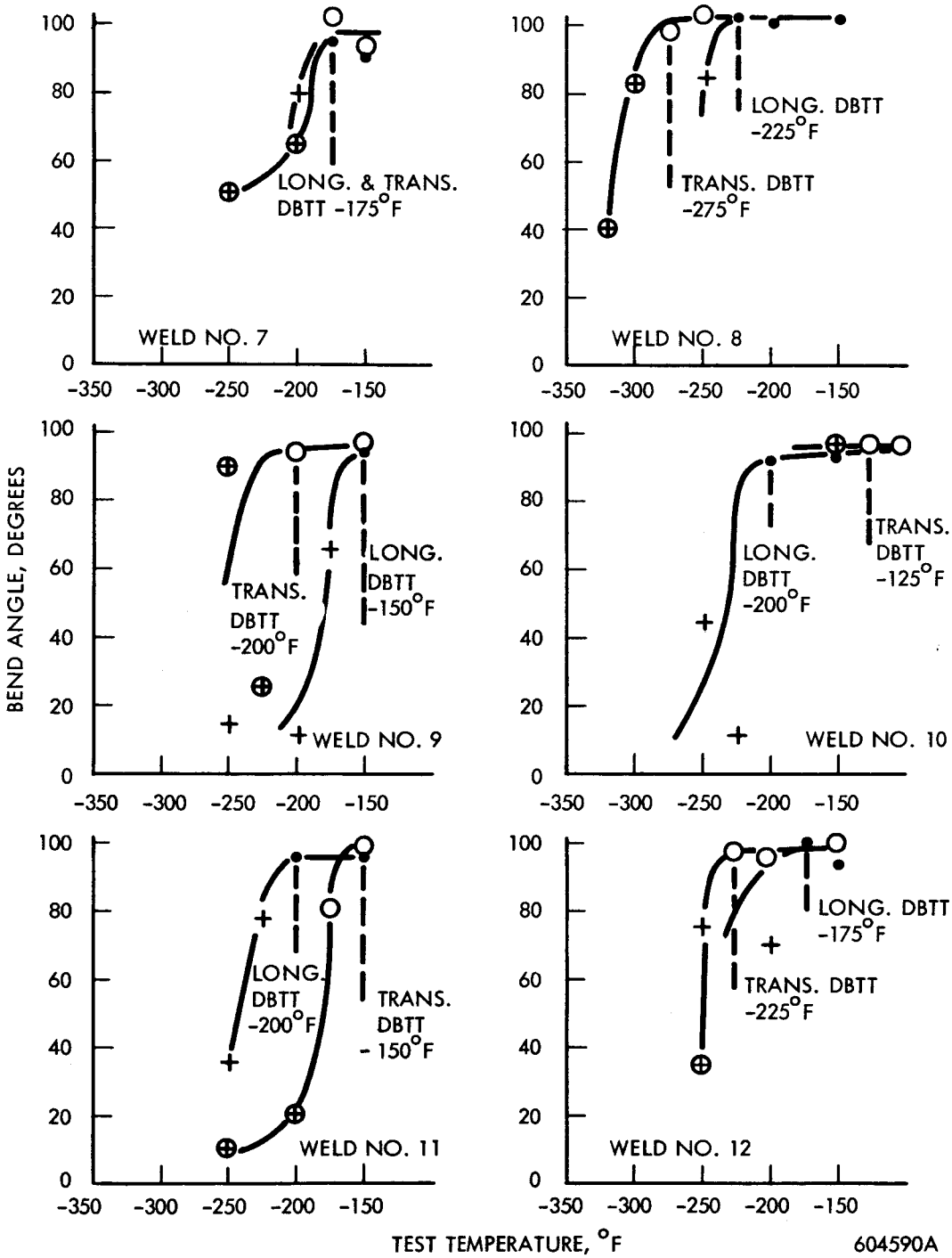

FIGURE 17 - SCb-291 TIG Weld Bend Test Results. 1t Bend Radius. For Weld Record See Table 11.

TABLE 11 - SCb-291 Sheet. TIG Butt Weld Record

Weld No.	Clamp Spacing (inch)	Speed (ipm)	Current Amperes	Weld Width Top/Bottom (inch)	Q Joules/Inch	Atmosphere Monitor Readings			Comments	
						O_2(1) ppm	O_2(2) ppm	H_2O(3) ppm	Visual Inspection	Dye Check
1	3/8	15	70	0.15/0.13	4,770	3.5	--	0.9	Negative	Negative
2	3/8	30	115	0.18/0.16	3,900	3.5	--	0.9	1/8" HAZ Crack	1/8" HAZ Crack
3	1/4	15	83	0.16/0.15	5,640	2.5	3.6	0.4	Edge Flash(4)	Negative
4	1/4	30	100	0.125/0.110	3,400	4.0	4.6	1.6	Edge Flash(4)	Negative
5	1/4	7.5	56	0.136/0.114	8,050	2.0	3.5	0.2	Negative	Negative
6	1/4	7.5	72	0.150/0.140	10,650	1.5	3.4	0.4	Negative	Negative
7	1/4	15	75	0.120/0.090	5,400	--	2.5	0.1	Negative	Negative
8	3/8	15	88	0.216/0.210	6,510	1.6	3.6	1.5	Negative	Negative
9	1/4	30	160	0.198/0.192	6,080	0.5	2.1	0.2	Negative	Negative
10	1/4	60	166	0.135/0.084	3,155	--	3.1	2.6	Negative	Negative
11	3/8	60	145	0.120/0.045	2,680	1.0	3.0	0.9	Negative	Negative
12	3/8	60	185	0.180/0.156	3,520	1.5	2.8	1.5	Negative	Negative

(1) Westinghouse Oxygen Gage
(2) Lockwood & McLorie Oxygen Gage
(3) CEC Moisture Monitor
(4) Instantaneous Arcing to Weld Clamp Down

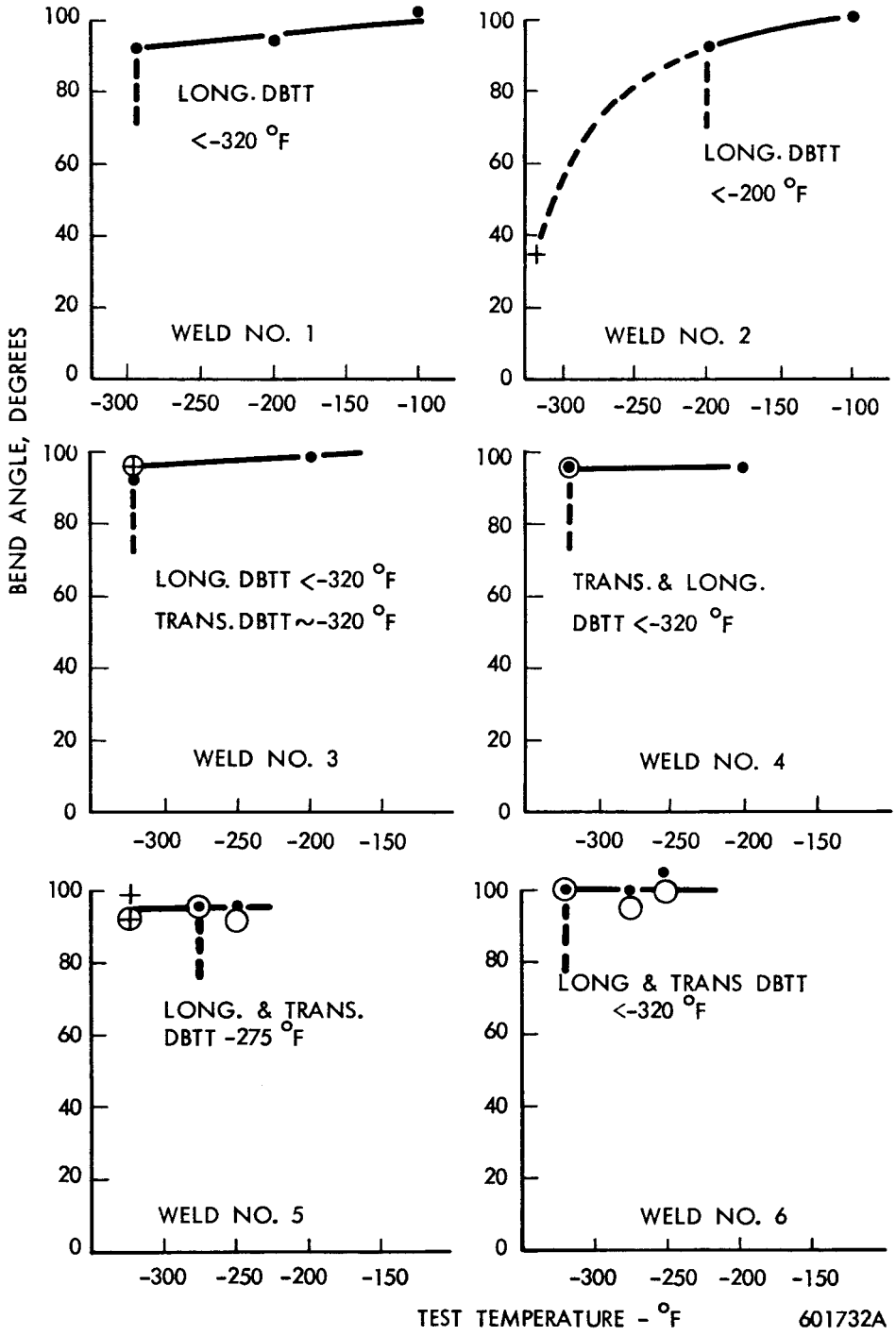

FIGURE 18 - Ta-10W TIG Weld Bend Test Results. 1t Bend Radius. For Weld Record See Table 12.

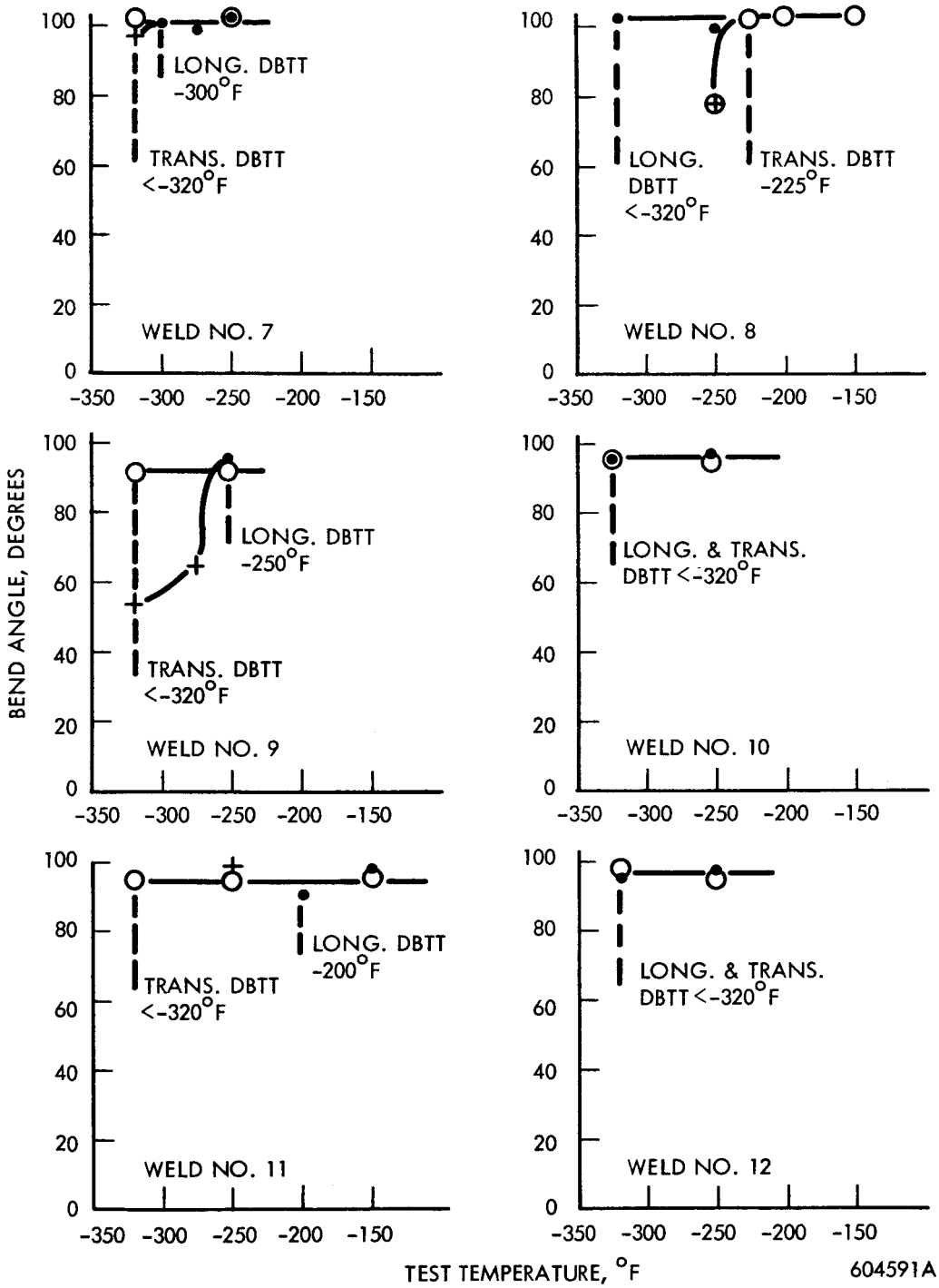

FIGURE 19 - Ta-10W TIG Weld Bend Test Results. 1t Bend Radius. For Weld Record See Table 12.

TABLE 12 - Ta-10W Sheet. TIG Butt Weld Record

Weld No.	Clamp Spacing (inch)	Speed (ipm)	Current Amperes	Weld Width Top/Bottom (inch)	Q Joules/Inch	Atmosphere Monitor Readings			Comments	
						O_2(1) ppm	O_2(2) ppm	H_2O(3) ppm	Visual Inspection	Dye Check
1	3/8	15	115	0.180/0.180	7,800	--	3.5	3.0	Negative	Negative
2	3/4	15	90	0.160/0.150	6,110	--	3.5	4.5	Negative	Negative
3	1/4	15	90	0.135/0.080	6,110	4.5	4.6	2.3	Negative	Negative
4	1/4	30	126	0.125/0.075	4,295	5.0	3.6	2.6	Edge Flash(4)	Negative
5	1/4	7.5	80	0.120/0.082	11,500	--	2.4	0.4	Negative	Negative
6	1/4	7.5	73	0.190/0.180	17,450	5.0	4.0	4.8	Negative	Negative
7	3/8	7.5	118	0.165/0.144	12,910	--	2.6	5.2	Negative	Negative
8	1/4	15	167	0.195/0.189	13,350	--	2.7	0.3	Negative	Negative
9	1/4	30	215	01195/0.189	8,160	--	1.7	3.3	Negative	Negative
10	1/4	60	255	0.165/0.150	5,350	1.5	3.4	0.2	Negative	Negative
11	3/8	60	230	0.165/0.150	4,370	1.5	3.6	1.1	Negative	Negative
12	1/4	60	215	0.150/0.096	4,080	1.5	3.7	1.2	Negative	Negative

(1) Westinghouse Oxygen Gage
(2) Lockwood & McLorie Oxygen Gage
(3) CEC Moisture Monitor
(4) Instantaneous Arcing to Weld Clamp Down

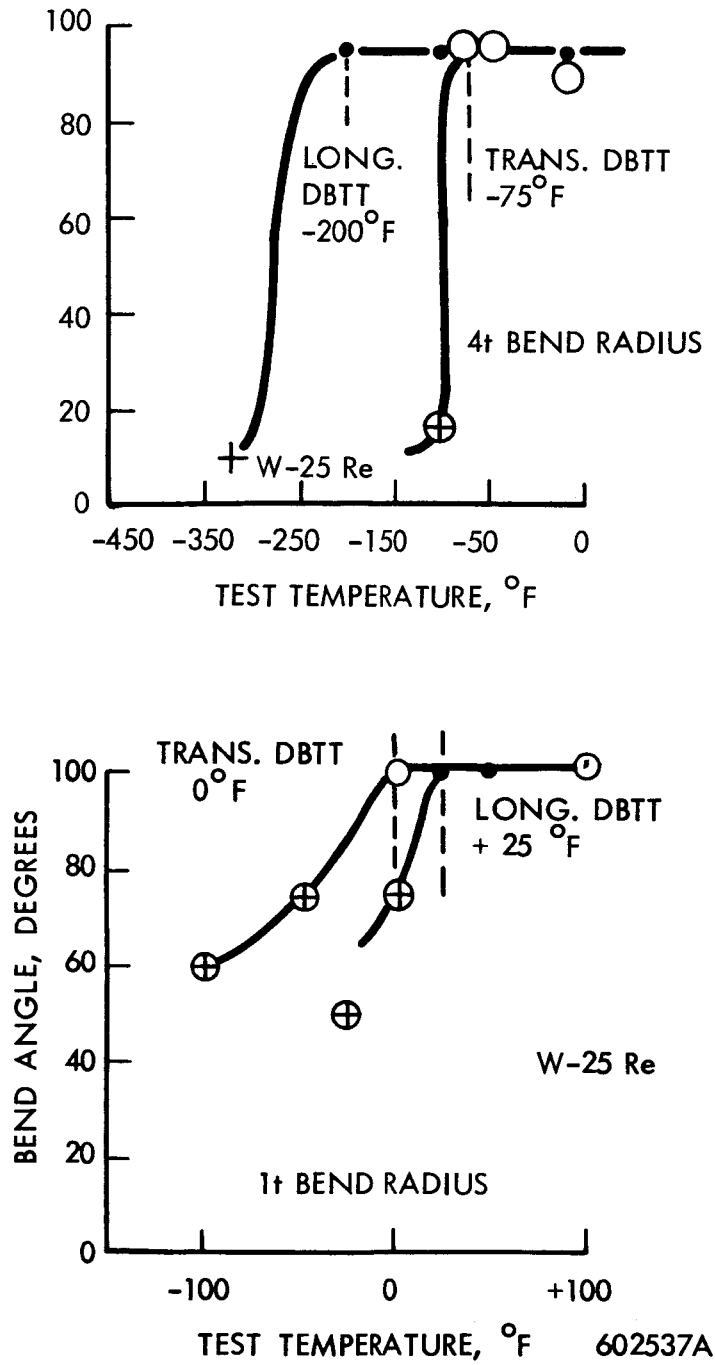

FIGURE 20 - W-25Re Base Metal Bend Test Results. Top,4t Bend Radius. Bottom,1t Bend Radius.

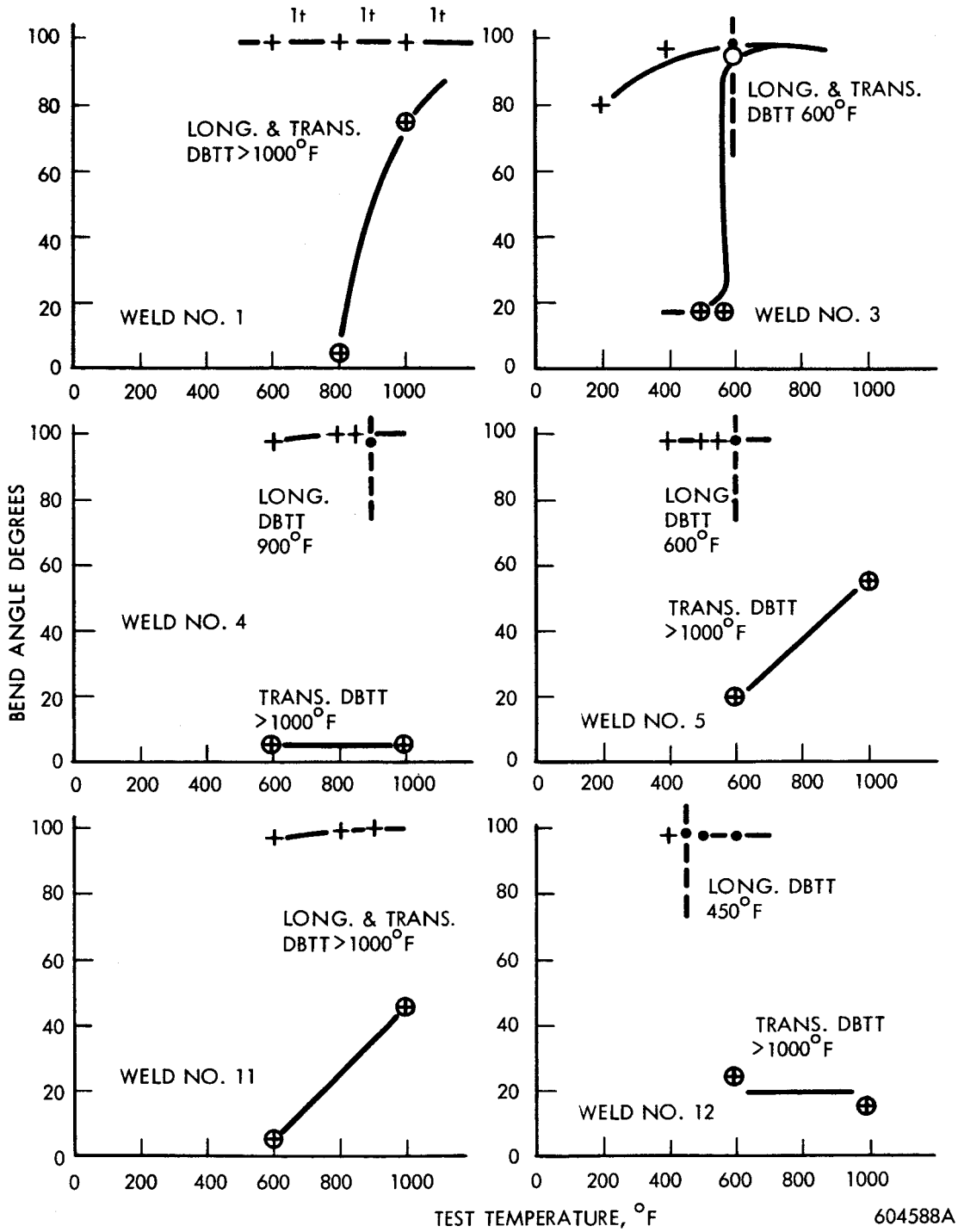

FIGURE 21 - W-25 Re EB Weld Bend Test Results. 4t Bend Radius. For Weld Record See Table 13.

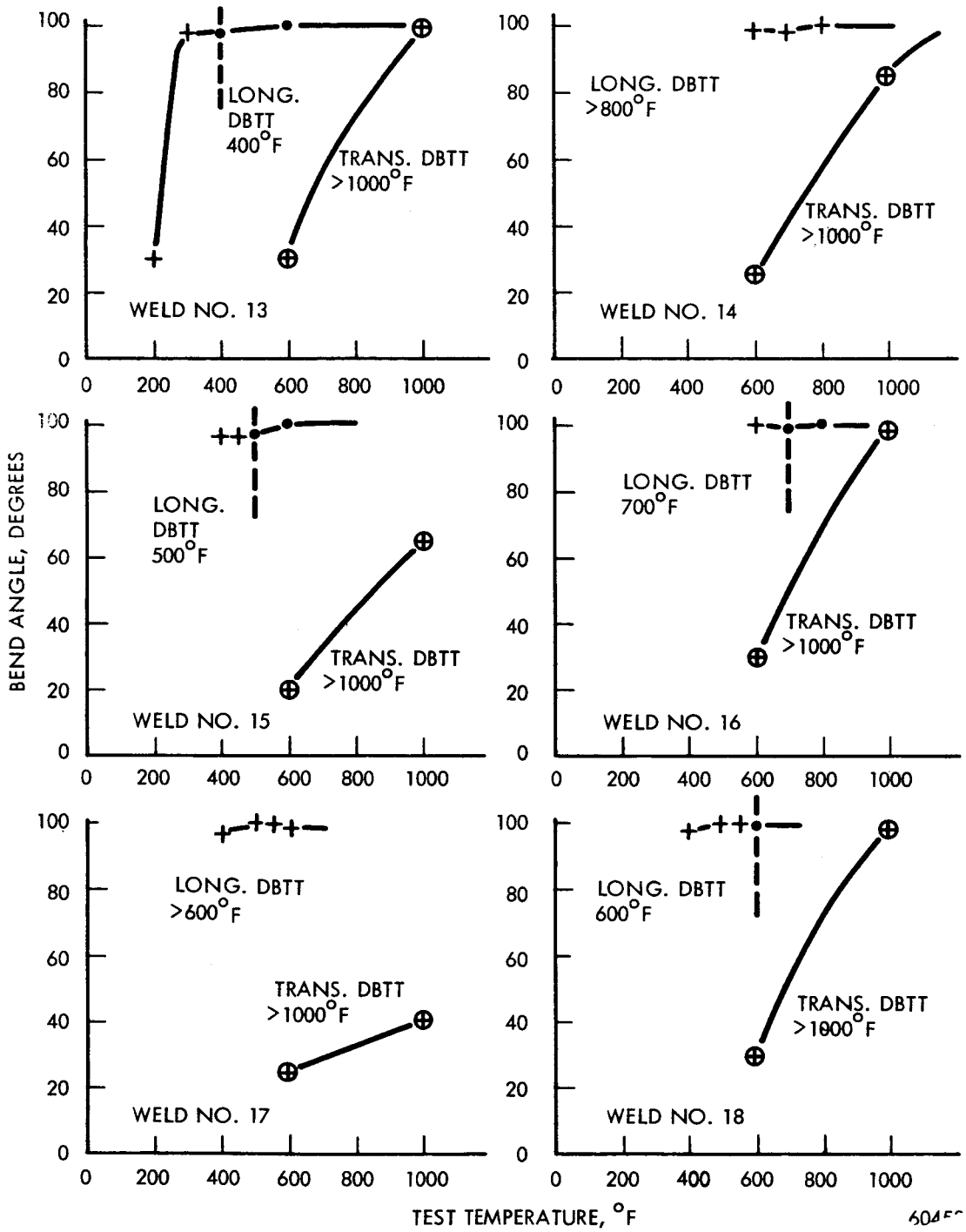

FIGURE 22 - W-25Re EB Weld Bend Test Results. 4t Bend Radius. For Weld Record See Table 13.

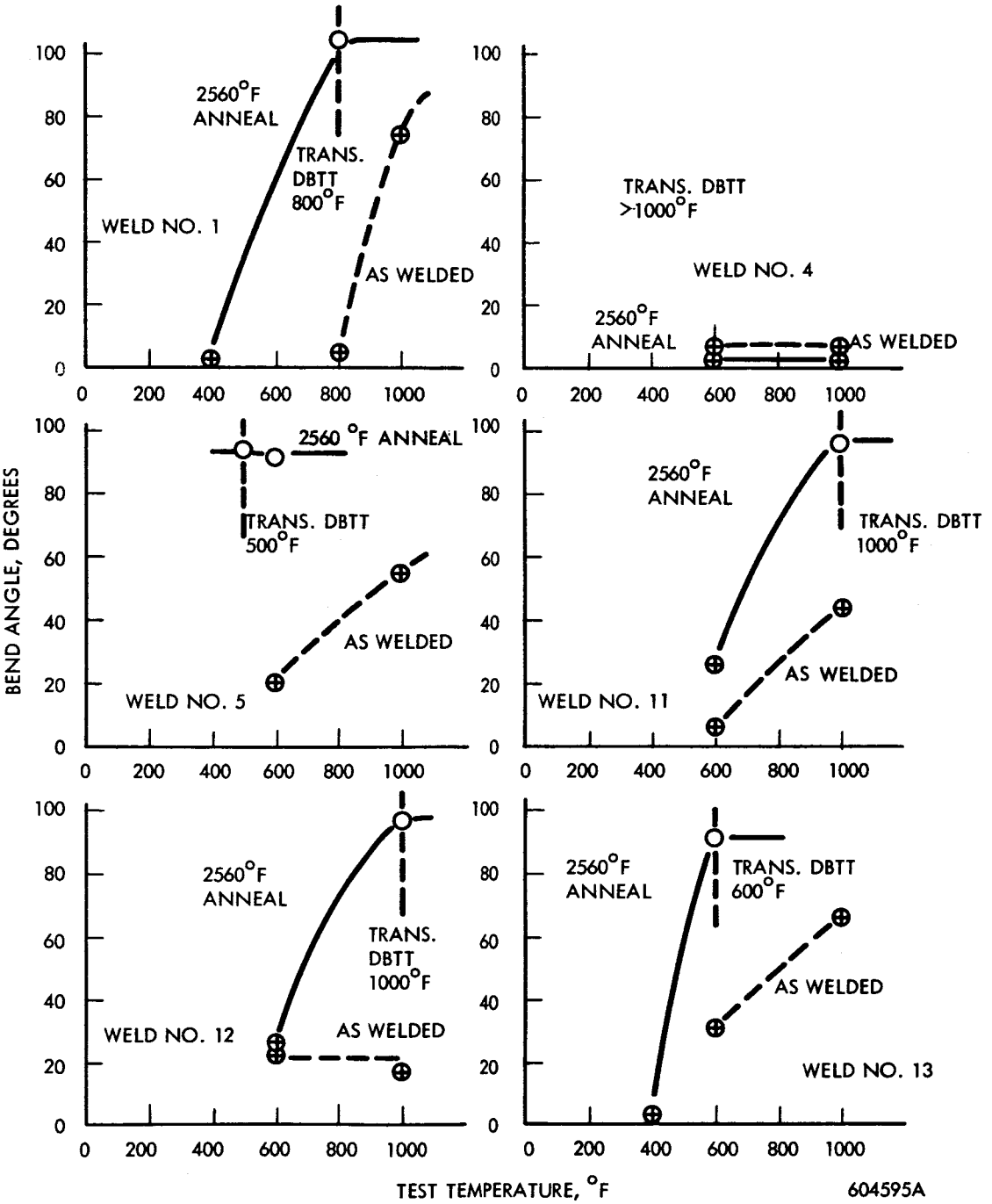

FIGURE 23 - Bend Test Results of W-25Re EB Welds Stress Relieved for One Hour at 2560°F. 4t Bend Radius. For Weld Record See Table 13.

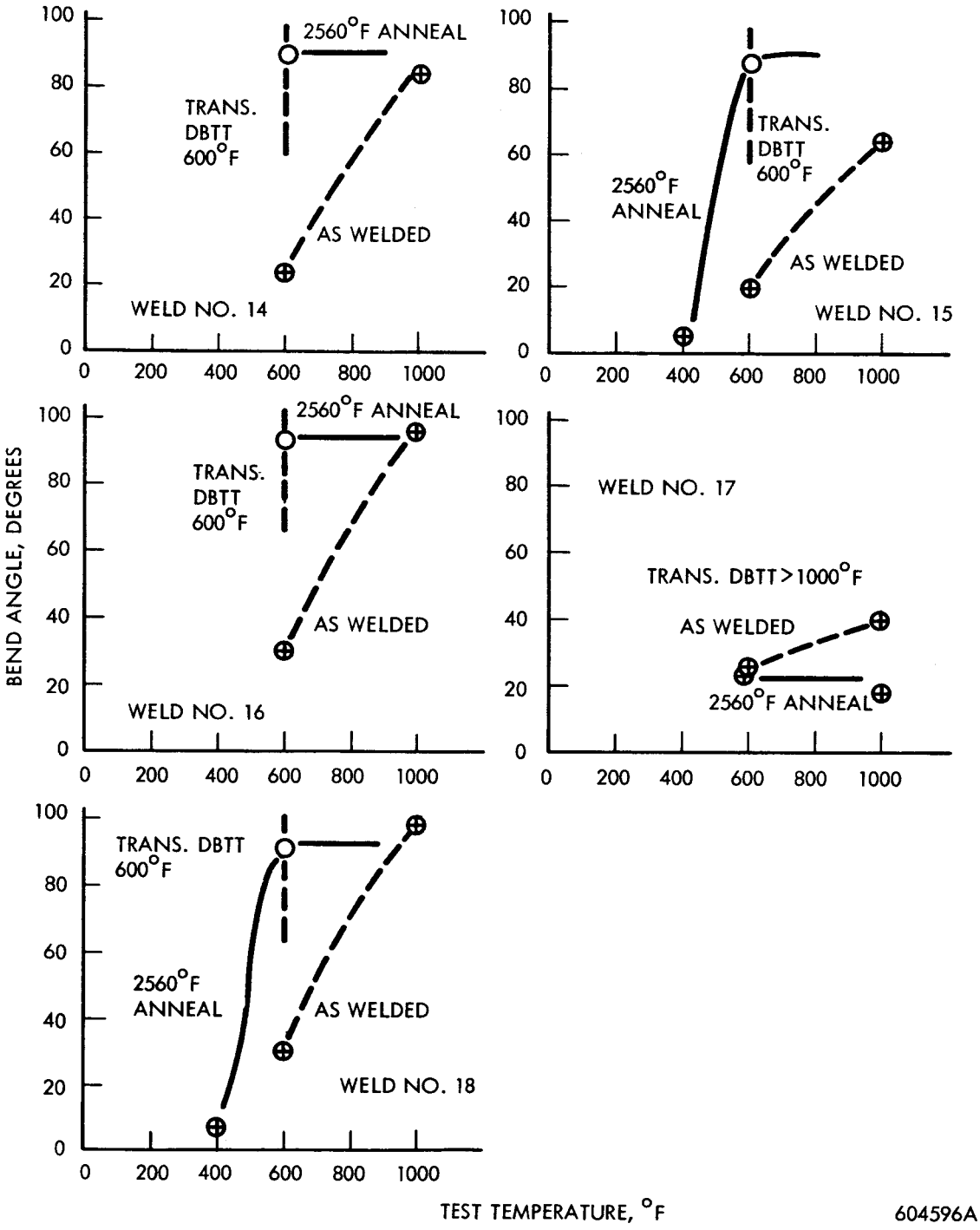

FIGURE 24 - Bend Test Results of W-25Re EB Welds Stress Relieved for One Hour at 2560°F. 4t Bend Radius. For Weld Record See Table 13.

TABLE 13 - Electron Beam Welding Parameters for W-25Re

Weld[3] No.	Speed (ipm)	Deflection[1] (inches)	Current (ma)	Chill Spacing (inches)	Power[2] (watts)	Watt-Sec. per inch	Weld Bead Width (inches)		Vacuum (torr)
							Top	Bottom	
1	100	L-0.050	7.5	0.250	1125	675	0.028	0.018	5.0×10^{-6}
3	50	L-0.050	6.3	0.250	945	1130	0.035	0.023	5.0×10^{-6}
4	100	L-0.050	7.2	0.094	1080	650	0.029	0.017	5.0×10^{-6}
5	50	L-0.050	6.0	0.094	900	1080	0.035	0.022	5.0×10^{-6}
11	50	zero	5.6	0.094	840	1010	0.027	0.020	1.7×10^{-6}
12	25	L-0.050	6.0	0.094	840	2010	0.040	0.032	1.7×10^{-6}
13	15	L-0.050	4.6	0.250	690	2860	0.036	0.022	2.0×10^{-6}
14	50	L-0.100	7.2	0.094	1080	1300	0.031	0.022	2.0×10^{-6}
15	50	L-0.025	6.0	0.094	900	1080	0.030	0.022	2.0×10^{-6}
16	15	L-0.050	5.1	0.094	765	3020	0.038	0.027	2.0×10^{-6}
17	15	zero	4.8	0.094	720	2880	0.032	0.023	2.0×10^{-6}
18	15	T-0.050	5.7	0.094	855	3420	0.060	0.050	2.0×10^{-6}

1. L. is longitudinal
   T. is transverse

2. All welds made at 150 KV

3. 18 welds were made to produce 12 acceptable welds because of a welding problem mentioned on Pages 13 and 14.

C. EQUIPMENT AND PROCEDURES

1. Aging Furnace Performance Evaluation

Three of the five ultra-high vacuum furnaces were operated for 500 hours to determine the pressure-time characteristics to be expected with a normal furnace load at various operating temperatures. Initial vacuum furnace operation was completely trouble free, providing an uninterrupted 500 hour run in each of the three furnaces. An expected high gas load was observed during initial furnace heating, following which the chamber pressure continually improved throughout the furnace run. Two furnaces operating at 2300°F and 2100°F with a tantalum alloy load reached the 10^{-9} torr range after four hours of operation. A third furnace was operated under the most difficult program conditions anticipated, 3200°F with a full furnace load. With supplementary titanium sublimation pumping, an ion gage pressure of 10^{-9} torr was obtained in this furnace after 10 hours of operation. Without sublimation pumping the 10^{-9} torr range was reached after 500 hours of continuous furnace operation. Figure 25 shows the pressure-operating time relationship of the three furnaces.

Ultra-High Vacuum Furnaces - These vacuum furnaces, shown in Figure 26, were manufactured by Varian Associates of Palo Alto, California. The following is a brief description of their specification and performance:

Furnace:

Location:	In throat of sputter ion pump
Hot Zone:	4 Inch diameter x 6 inch long
Heater:	Tantalum split tube resistance
Radiation Shields:	4 concentric, 0.002 inch tantalum
Cold Wall:	Water cooled OFHC copper
Capability:	3200°F at 9KW - 2100°F at 1.8KW

Pumping System:

Roughing:	Initial pumpdown to 5×10^{-3} torr is accomplished by a series of three liquid nitrogen cooled molecular sieve sorption pumps.
High Vacuum Pumping:	500 l/sec. diode sputter ion pump

Auxiliary pumping can be provided by attaching a titanium sublimation pump cartridge or element to any of the furnace service ports.

Pressure Measurement:	Bayard-Alpert Gage (2×10^{-11} torr)

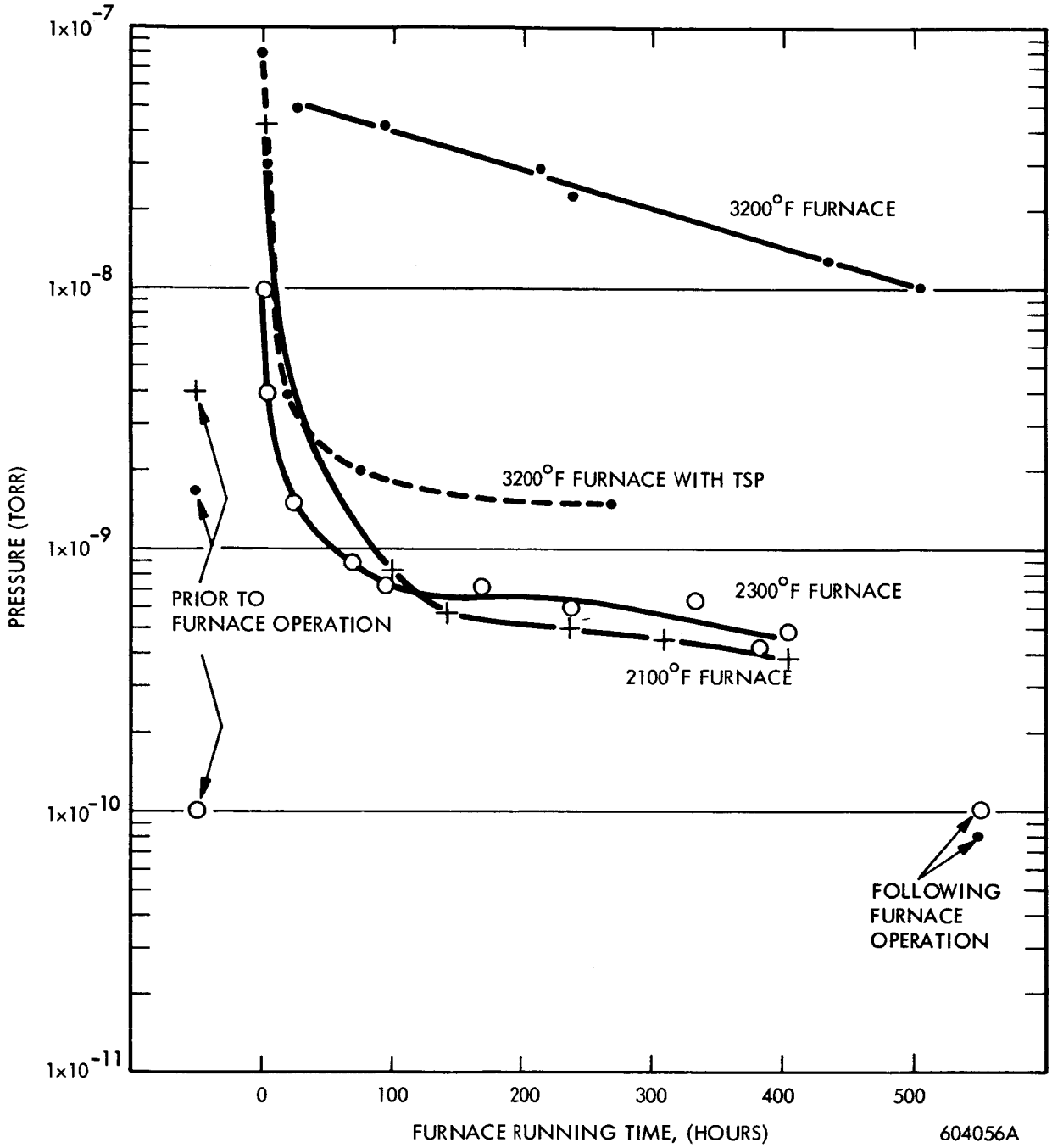

FIGURE 25 - Ion Gage Pressure-Time Characteristics For Three Furnaces

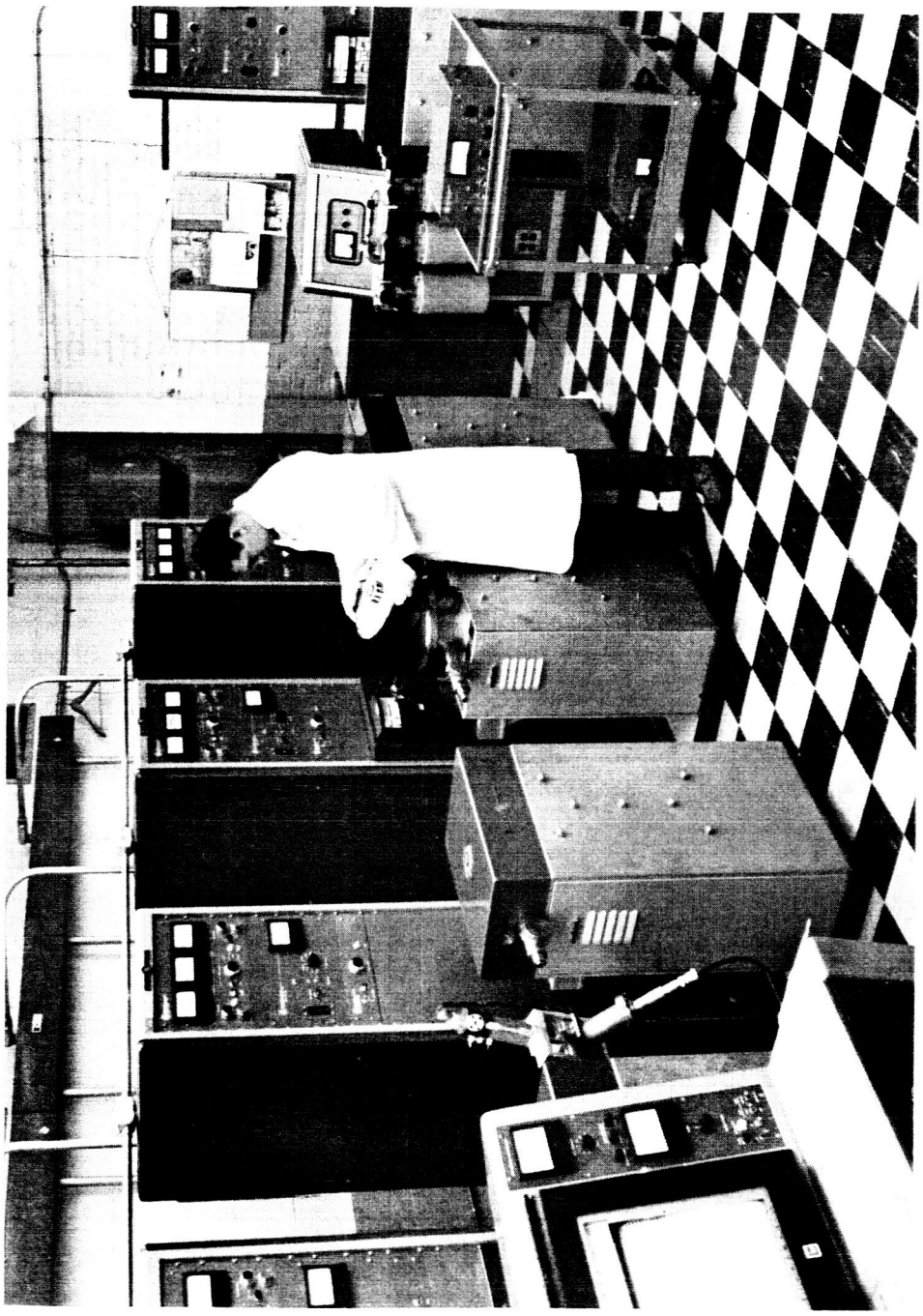

FIGURE 26 - Ultra-High Vacuum Annealing Laboratory

System Capabilities:

Empty Cold Furnace After 24 Hours:		1×10^{-8} torr
Baked Empty Cold Furnace After 24 Hours:		1×10^{-9} torr
2100°F:	After 1 Hour	1×10^{-8} torr
	After 100 Hours	1×10^{-9} torr
	After 240 Hours	5×10^{-10} torr
3200°F:	After 30 Hours	5×10^{-8} torr
	After 500 Hours	1×10^{-8} torr

With Titanium Sublimation Pumping at 3200°F:

After 5 Hours	3×10^{-8} torr
After 10 Hours	1×10^{-8} torr
After 22 Hours	4×10^{-9} torr

Residual Gas Analysis - A Veeco magnetic sector residual gas analyzer was attached to the furnace operating at 3200°F to observe changes in the residual gas composition as the furnace run progressed. A description of the GA-3 analyzer is provided in Table 14. Figure 27 shows the position of the appendage analyzer head on the furnace chamber. Analyses were made following a 450°F system bakeout and throughout the furnace run, including the period of higher pressures encountered during furnace heat up.

Gas species sensitivity values supplied by the manufacturer were used to convert the residual gas analyzer scale readings to partial pressures. A leak valve has been obtained to permit in situ calibration on the ultra-high vacuum furnaces. Until such data is obtained, the manufacturers reference figures will be used. Of equal importance to the pressure-sensitivity calibration of the mass spectrometer is the calibration of the total system pumping speed. Sputter ion pumps in general, and systems containing heated reactive metals in particular, show marked preferential chemical pumping for certain gas species, particularly nitrogen and oxygen. In other words, a substantial air leak could be masked from both the ion gage and the residual gas analyzer by efficient pumping of the furnace load, and this condition can be revealed using a leak of known size.

Several mass peaks commonly encountered in ultra-high vacuum work can be composed of several gas species. This factor was considered in analyzing the data presented in this report. Mass/charge ratio or mass peak 28, for instance, can be N_2, CO, Si, or C_2H_4 in which case the cracking patterns of the possible gases are used to determine the major peaks. The double ionized nitrogen peak at 14 is used to distinguish between nitrogen and carbon monoxide of peak 28, and

TABLE 14 - VEECO GA-3 Data Sheet

Vacuum-Electronics Corp. GA-3 UHV Residual Gas Analyzer	
MASS SPECTROMETER TUBE	Stainless steel, flange-mounted, 60° Nier type mass spectrometer tube bakeable to 400°C. Source and collector assemblies are removable and self-aligning. Permanent joints are Nicrobrazed. Flanged connections utilize positive seal gold gasketing.
MASS RANGE	2-90 a.m.u. covered in two increments: 90-10 and 12-2.
RESOLUTION	44 at mass 44 (width measured at 1% peak Height)
SENSITIVITY	Partial pressure of 1×10^{-10} torr or less for nitrogen.
PRESSURE RANGE	10^{-4} to 10^{-10} torr.
MAGNETIC FIELD	Permanent magnet and pneumatically-operated shunt.
AMPLIFIER	Ultra-stable Veeco electrometer amplifier has a minimum detectable signal of 2×10^{-15} amp. with unit signal-to-noise ratio. First stage amplification is provided at the signal source by a hermetically-sealed remote probe, mounted directly on the collector end of the mass spectrometer tube.
RECORDER	Special three decade linear Leeds and Northrup Speedmax "G" potentiometer records, 100 millivolt full scale; shart speed of 2" per minute; mounted in the console.

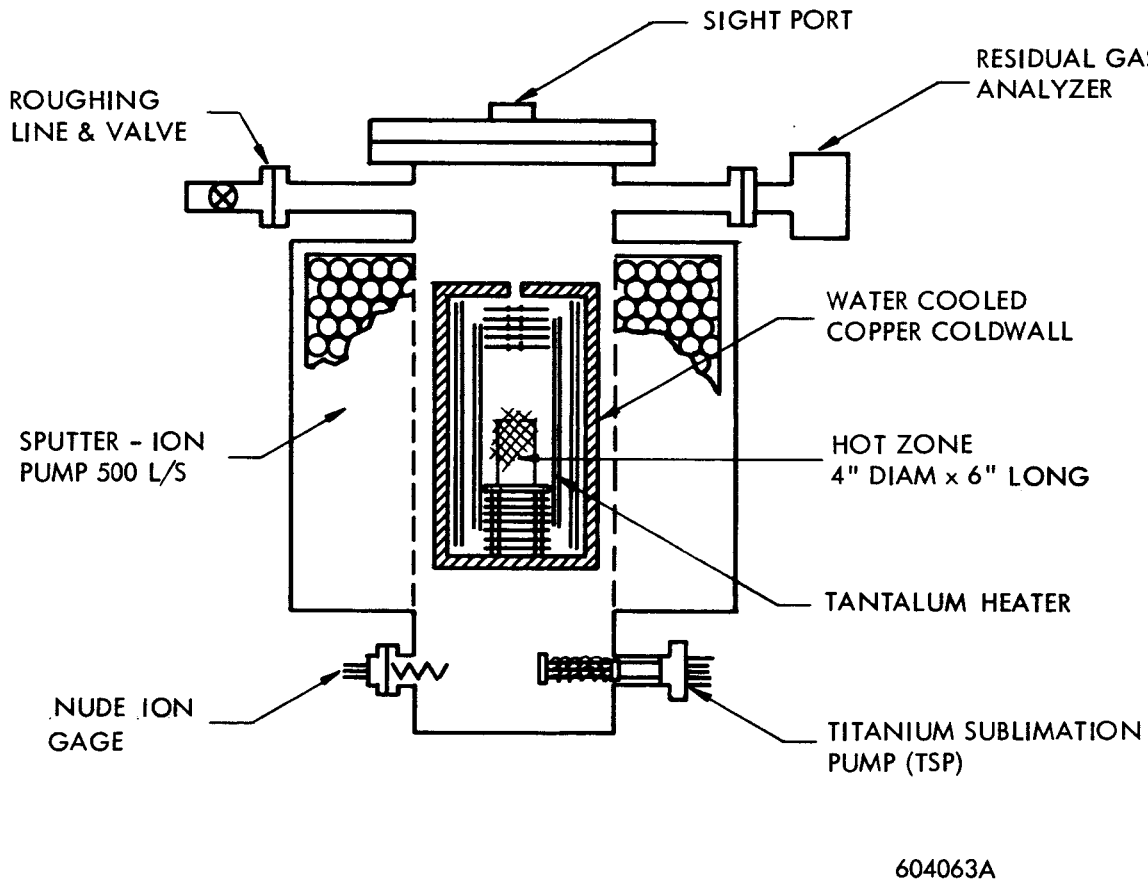

FIGURE 27 - Internal Arrangement of Ultra-High Vacuum Furnace

and likewise the peak of C_2H_4 at 28 is related to its complementary peak 27. The cracking patterns supplied by the manufacturer were used in evaluating the residual gas analyzer scans. Again, this represents the best information available, but may not be strictly applicable in the highly reactive and ionizing environment of the vacuum furnace. Typical plots of the species partial pressures are shown in Figures 28 and 29 which represent the residual gas composition prior to and following a 500 hour, 3200°F furnace run. A continuous plot of partial pressures of selected gas species is shown in Figures 30, 31, and 32 as a function of furnace operating time.

Hydrogen was largely responsible for the initial high gas load. The hydrogen level, Figure 30, dropped following initial heat up and carbon monoxide became the major residual gas species after the first 10 hours of operation. Helium and neon were not measureable prior to furnace operation, but rose to a high value during the initial furnace start up. During furnace operation, the partial pressures of helium, neon, and argon steadily fell, indicating efficient pumping action by the sputter ion pump.

Titanium Sublimation Pumping - The performance of an auxiliary titanium sublimation pump (TSP) was also evaluated during the 3200°F furnace run. The TSP was installed in the chamber bottom as shown in Figure 27. TSP operation was initiated during the initial heating cycle and continued for 22 hours after which the furnace performance was evaluated both with and without TSP. Figure 33 shows the TSP operating periods in detail. Since essentially two furnace performance tests were simultaneously run, (normal sputter ion pumping and titanium sublimation pumping) the pressure-time curves shown in this figure may be biased from completely separate tests.

The TSP was run in a nude operating position in the bottom well of the vacuum furnace. The surrounding chamber interior was used as the pumping surface providing considerably improved conductance over that which would normally be obtained with an appendage TSP chamber. A tantalum foil shield was used to protect the nude ion gage from line of sight exposure to sublimed titanium.

The TSP produced a dramatic decrease in pressure as measured by three pressure sensing devices: ion gage, residual gas analyzer, and ion pump current. The great change in ion gage reading is probably due to a significant local pressure decrease in the furnace bottom due to effective pumping of the titanium coated walls surrounding the ion gage. Residual gas analysis scans with and without the TSP operating showed no exceptional compositional changes, all gas species being reduced by the sublimation pump. Since both the TSP and the sputter ion pump operate by the same process, chemically combining and entrapping gas species in layers of titanium, such results would be expected.

Furnace Load Evaluation for 3200°f, 500 Hr. Run - One purpose of the 3200°F practice anneal was to determine the extent of specimen diffusion bonding

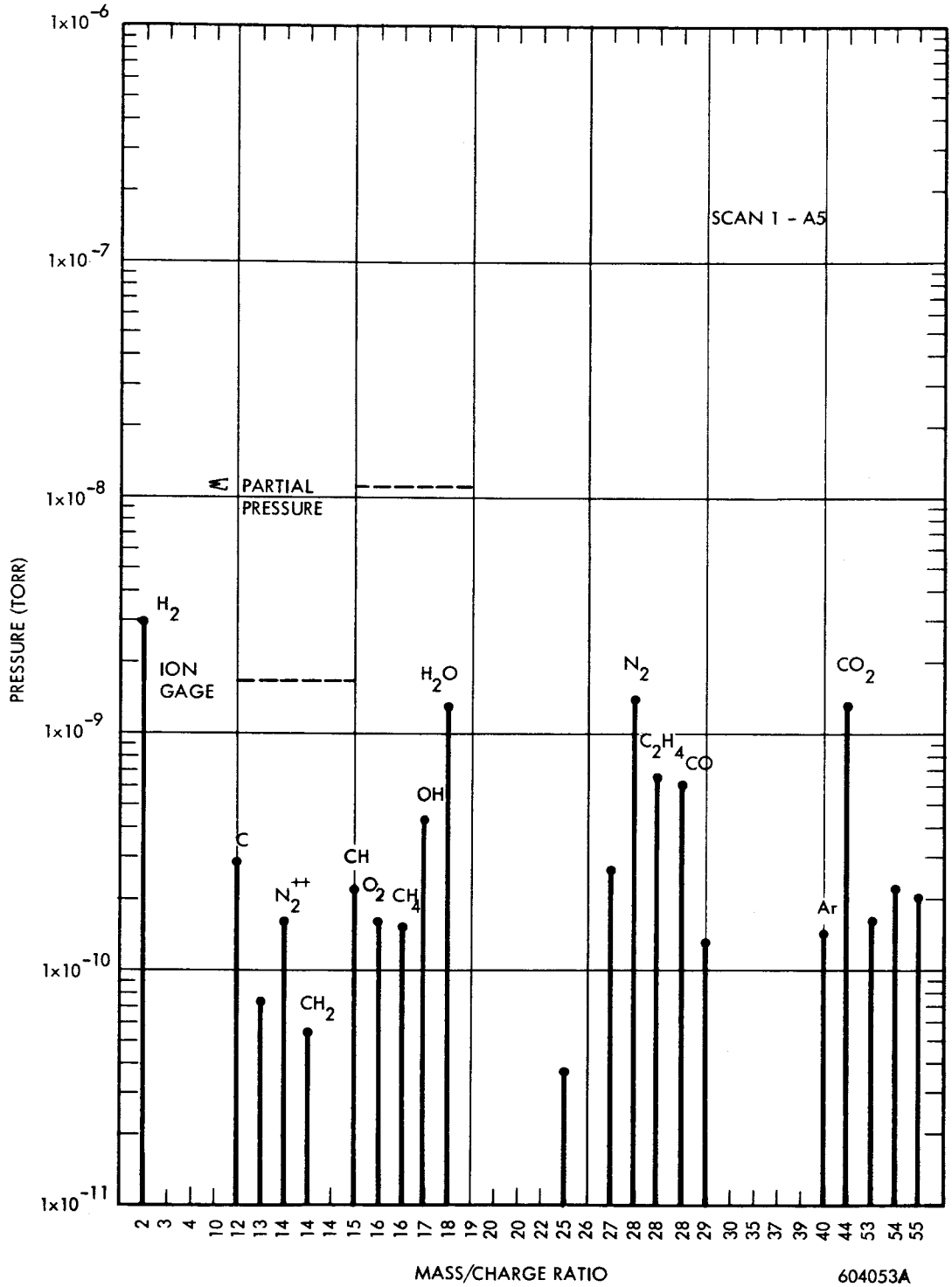

FIGURE 28 - Residual Gas Analysis Scan Prior to Furnace Operation

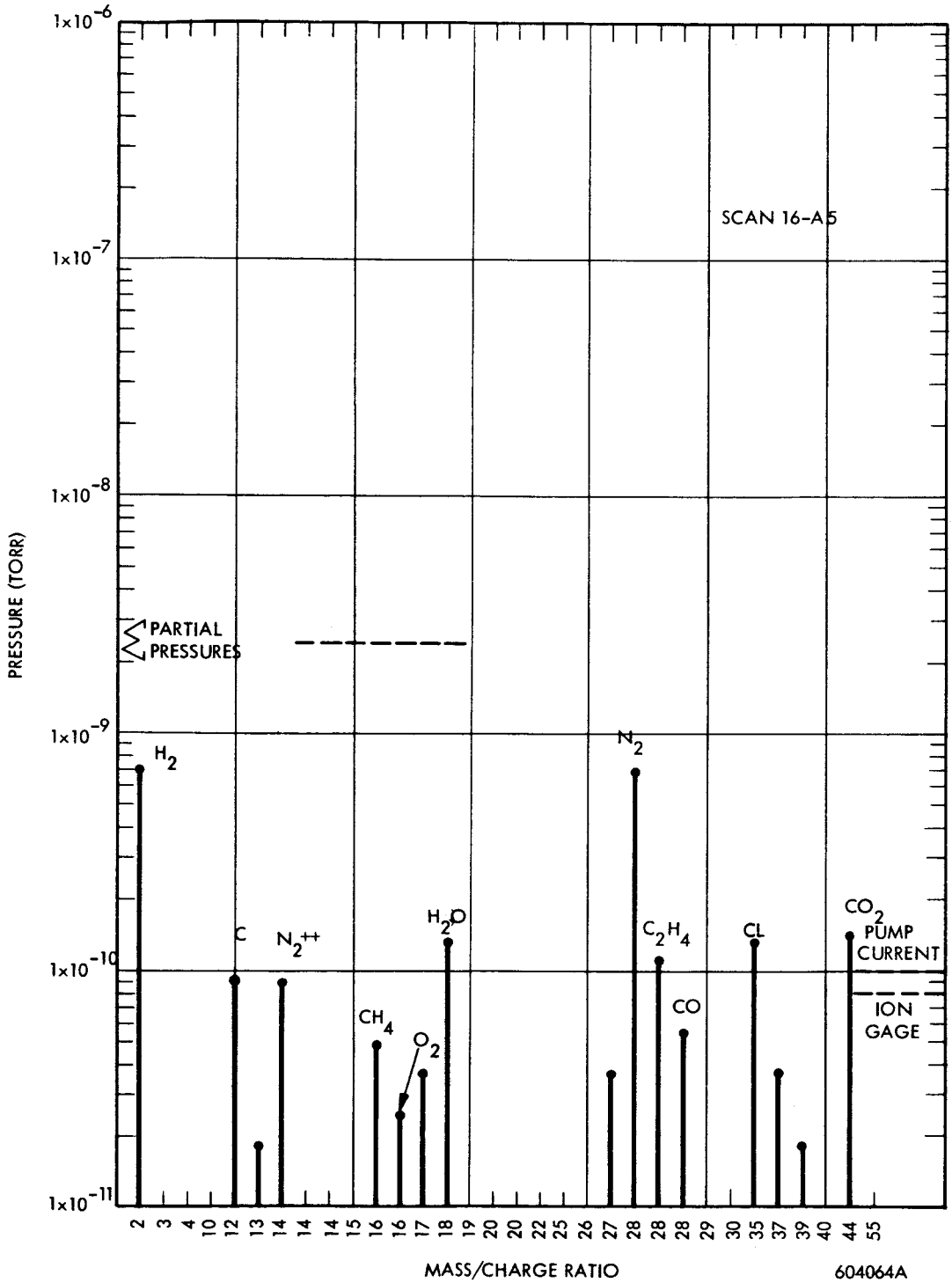

FIGURE 29 - Residual Gas Analysis Scan Following Furnace Operation

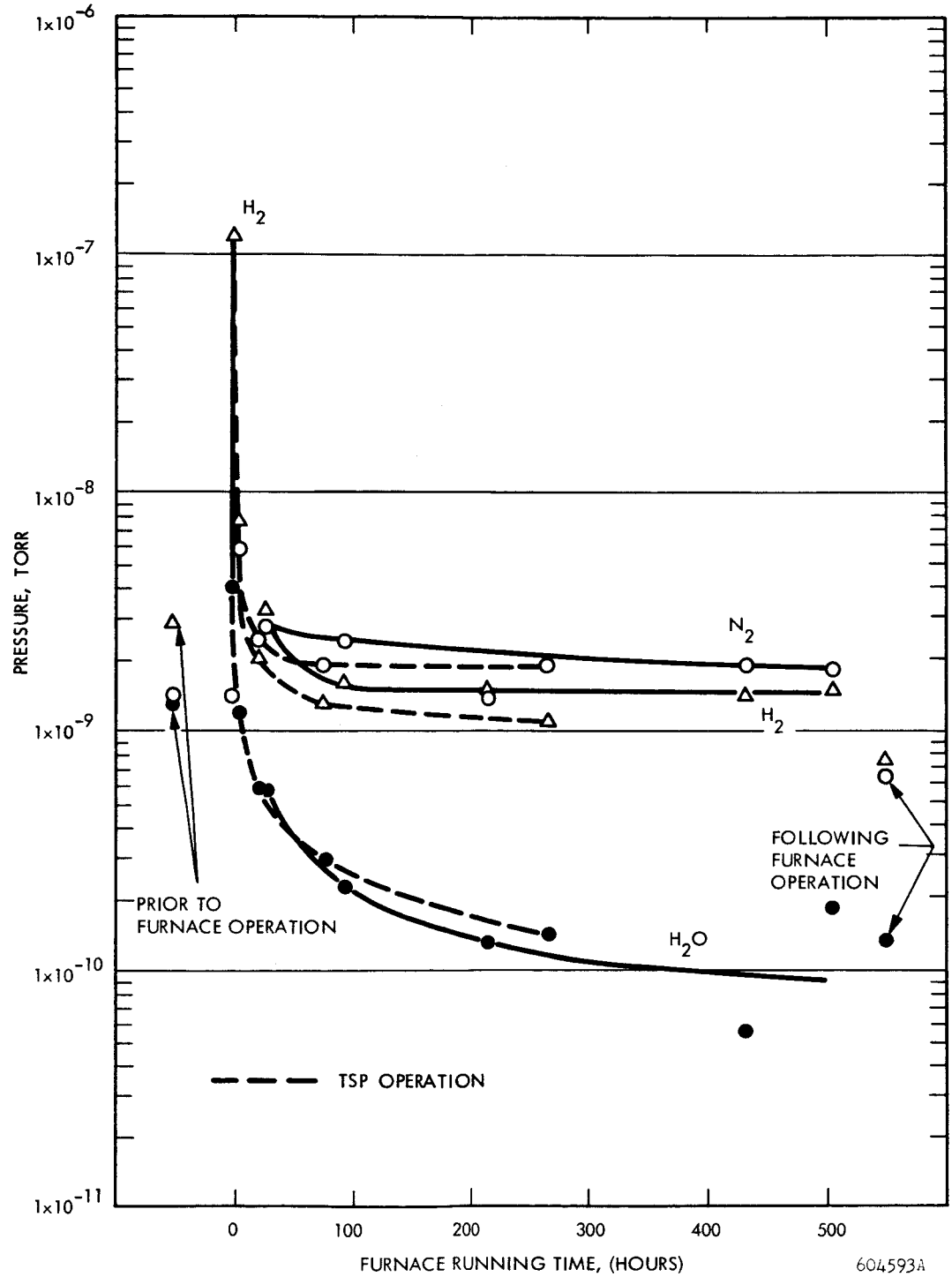

FIGURE 30 - 3200°F Furnace Partial Pressure-Time Characteristics for N_2, H_2, and H_2O

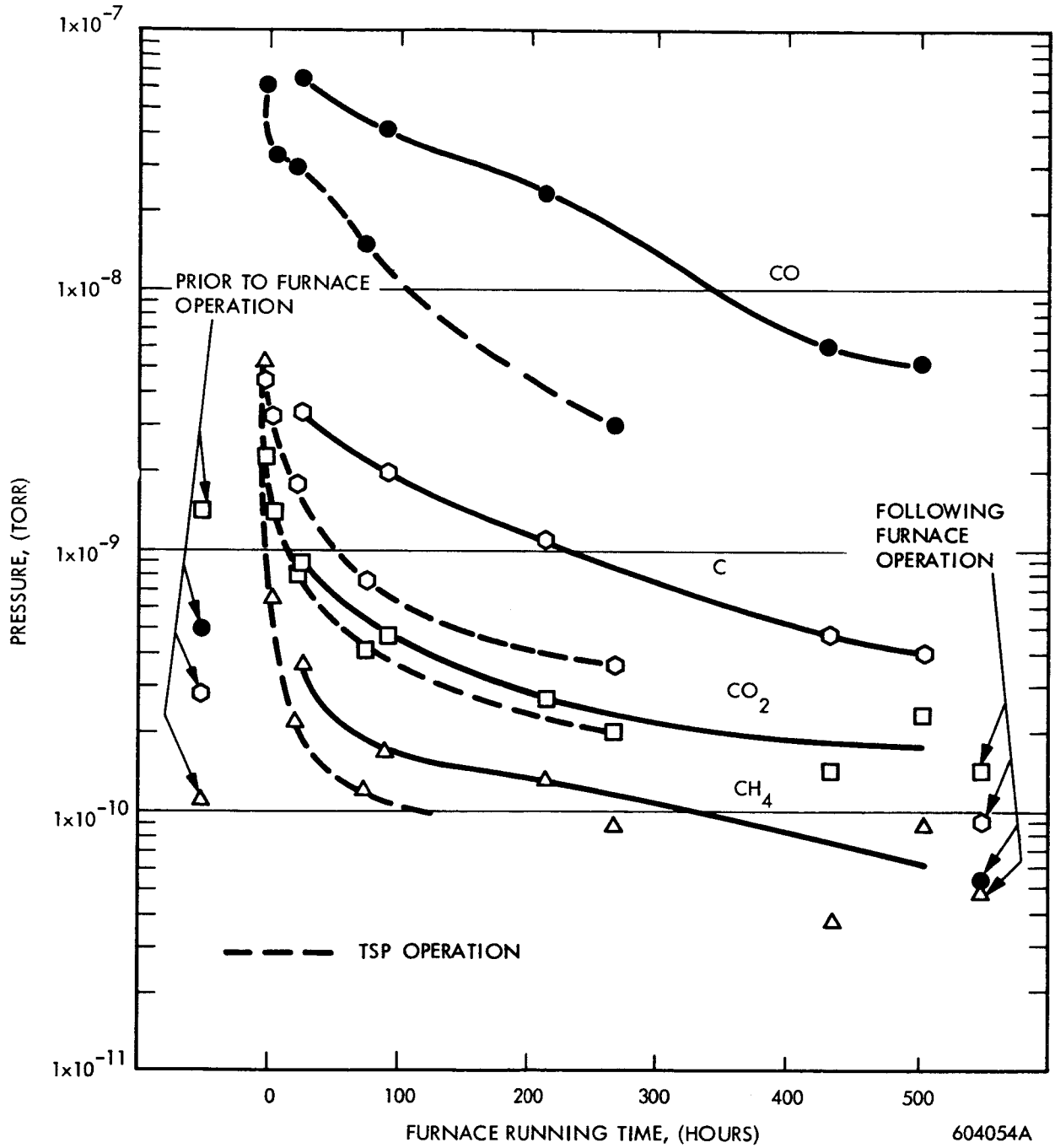

FIGURE 31 - 3200°F Furnace Partial Pressure-Time Characteristics for CO_2, CO, C, and CH_4

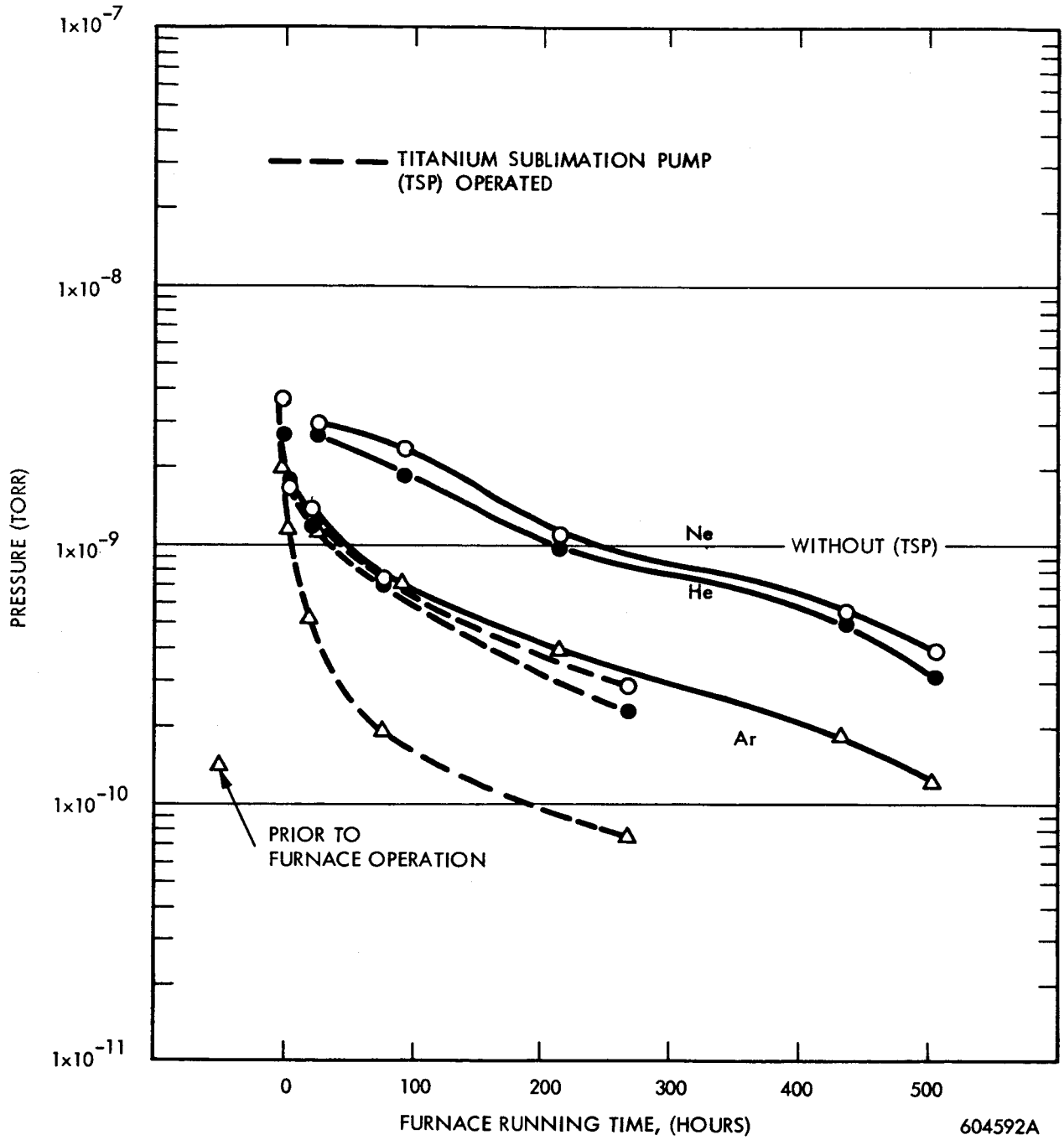

FIGURE 32 - 3200°F Furnace Partial Pressure-Time Characteristics for He, Ne, and Ar

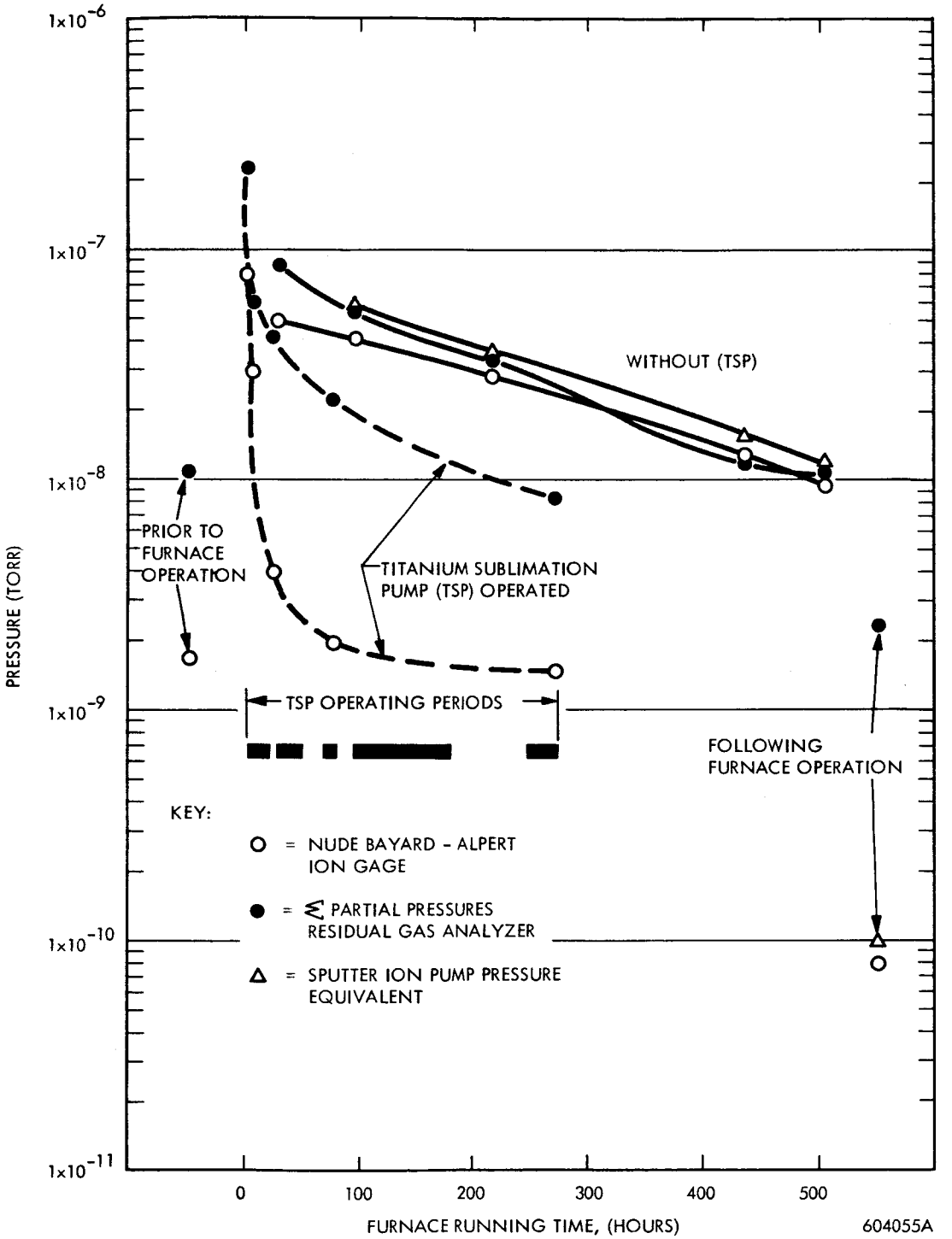

FIGURE 33 - 3200°F Furnace Pressure-Time Characteristics

which would occur at this temperature under ultra-high vacuum conditions. To provide some immediate answers to these questions, a dummy furnace load of various refractory metal alloys was included in the 3200°F furnace run. Groups of specimens of several alloys were wrapped together in tantalum foil and the entire furnace load was wired together with tantalum wire and set on the furnace platen. Specimens were wrapped both in face-to-face contact and with 0.010 inch diameter tantalum wire spacers.

Following the 500 hour heat treatment, the entire packet of specimens was lightly bonded together and to the tantalum furnace platen. A screwdriver and hammer sufficed to remove the specimen bundle from the platen and the individual alloy packets were separated with increasing difficulty from the top to the bottom of the bundle, the increased weight load at the bottom apparently producing a noticeable increase in bonding. Figure 34 is a photograph of the furnace load after heat treatment. Other than a tendency for the tantalum protective foil to bond to all alloys and itself, no significant difference was noticed between the bonding tendencies of the columbium alloys and T-222, the one tantalum alloy. W-25Re showed no tendency to bond to itself. A one pound piece of pure molybdenum included in the load formed a brittle alloy with the tantalum foil which was easily removed. The tantalum wire separators used between the bend test samples bonded to the columbium alloys leaving small depressions when removed. The wires did prevent specimen to specimen bonding and its attendant greater difficulties in separation. All the specimen-specimen bonding observed occurred at a very few contact points, but the strength of the bonds was great enough to often require specimen distortion and tearing for separation.

Following is a list of the alloys included in the test and a summary of the sticking problems observed:

Cb-Unalloyed	Foil to specimen and some specimen to specimen bonding.
Cb-1Zr	Foil to specimen and severe specimen to specimen bonding.
Cb-5Ti-1Zr-1Hf	Foil to specimen and very severe specimen to specimen bonding.
B-33 (Cb-5V)	Foil to specimen and very severe specimen to specimen bonding.
B-66 (Cb-5V-5Mo-1Zr)	Foil to specimen and light specimen to specimen bonding.
D-43 (Cb-10W-1Zr-.1C)	Foil to specimen, (slight) but no specimen to specimen bonding.

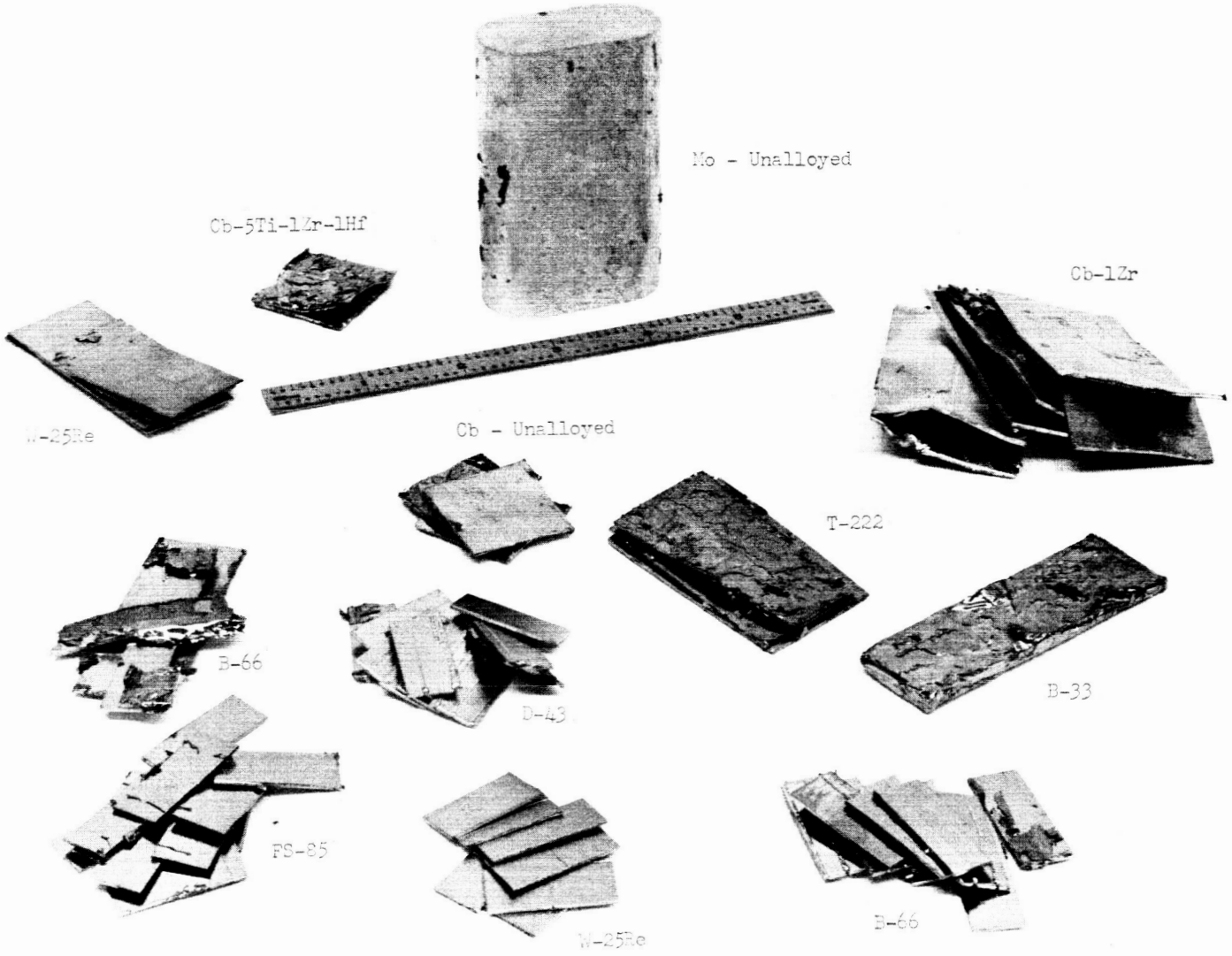

FIGURE 34 - Dummy Furnace Load After 500 Hours at 3200°F

FS-85 (Cb-10W-27Ta-1Zr)	Foil to specimen and light specimen to specimen bonding.
W-25Re	Foil to specimen (slight) but no specimen to specimen bonding.
Mo-Unalloyed	Foil formed brittle alloy with Mo and no data on specimen to specimen bonding.
Effect of Lower Temperature	Tantalum alloy samples heat treated for 500 hours at 2300°F showed no sticking problems, either to themselves or to the tantalum protective foil. Bonding of the foil to itself did occur.

This test demonstrated that long time, high temperature (3200°F) heat treatment in ultra-high vacuum environment results in specimen to specimen bonding of columbium and tantalum alloys. Complete specimen separation by wire or rod suspension is desirable but is not a particularly practical solution to this problem. Wire separation can be used if the small grooves produced by the wire can be tolerated. Tantalum foil readily bonds to itself, and to all the alloys tested, and should therefore perhaps not be used. A single layer of tantalum foil used as a contamination barrier could be used to cover the entire specimen package with only sacrificial specimens in actual contact with the foil.

2. Thermocouple Feed-Through Brazing

Platinum, platinum-10% rhodium thermocouples and tungsten-5% rhenium, tungsten-25% rhenium thermocouples have been selected for monitoring the anneal-ine furnace temperatures during the thermal stability studies. These will penetrate the high vacuum system through small diameter thin walled nickel tubes. The furnace feed-through assembly consists of eight nickel tubes permitting introduction of four thermocouples into each furnace. The tubes are brazed to a ceramic insulator.

The 82-18 gold-nickel brazing alloy was selected for joining the thermo-couples to the nickel tubulations. The brazing arrangement selected for this is shown in Figure 35. The bare thermocouple lead is passed through the nickel tube and is held in place for brazing by crimping the nickel tube at the braze location. The braze alloy, in the form of 0.010 inch diameter wire, is preplaced by wrapping at the joint location. The brazement is inserted in an argon purged vycor brand tube to provide shielding during brazing. The brazing is accomplished by induction heating the joint to the braze temperature, 1742°F, holding for

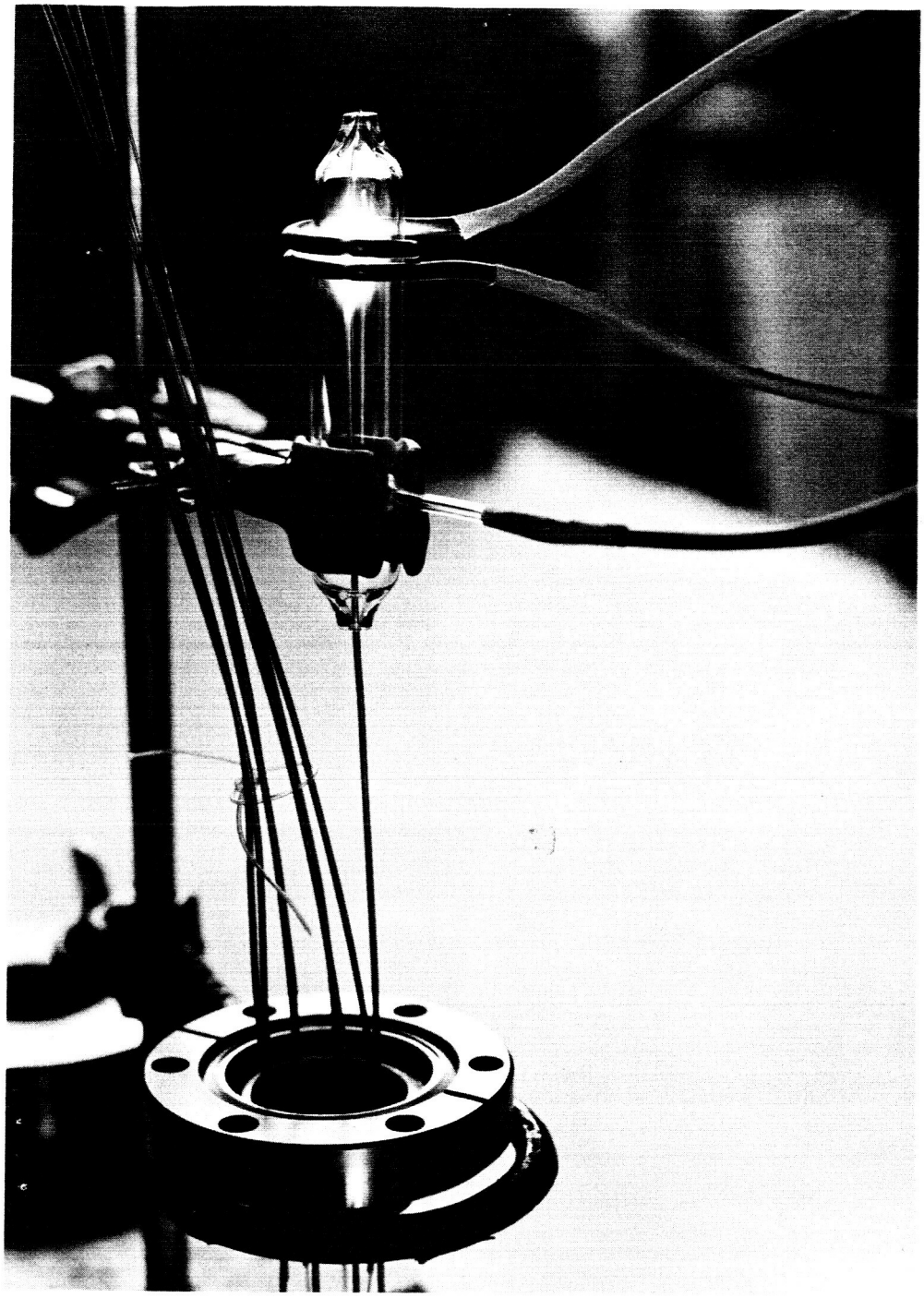

FIGURE 35 - Arrangement for Furnace Thermocouple Feedthrough Brazing

several seconds, and cooling. Induction brazing in this application has the advantages of providing localized heating and easy inert shielding.

3. Weld Chamber Glove Tests

Latex natural rubber gloves were functionally tested for oxygen and water vapor permeability. The welding chamber was normally evacuated, backfilled with helium, and oxygen and water vapor levels were monitored.

The natural rubber gloves released a considerable quantity of rubbery substance during the low pressure (10^{-6} torr) and moderate temperature (150-200°F) evacuation-bakeout cycle. The coating covered the relatively cool outer walls of the vacuum chamber and was removed with oxylene solvent. The latex natural rubber gloves apparently contain a high vapor pressure component which is released in quantity during the evacuation cycle and for this reason this glove material will not be used in the welding program.

The oxygen permeability was greater than any gloves tested, producing a chamber oxygen content rise to 22 ppm in 4 hours. Figure 36 compares the performance of the latex natural rubber gloves to the three other types of gloves tested in the program.[1] Figure 37 compares the water vapor permeability of the natural rubber gloves to the glove material tested earlier in the program.[1] Although the initial moisture reading was high, the rate of increase is normal.

In view of the results of the latest glove tests of natural rubber, cement neoprene still appears to be the most satisfactory material. The combination of low permeability to both oxygen and water vapor, adequate electrical insulation properties for manual welding and satisfactory vacuum stability is better than for the other materials tested.

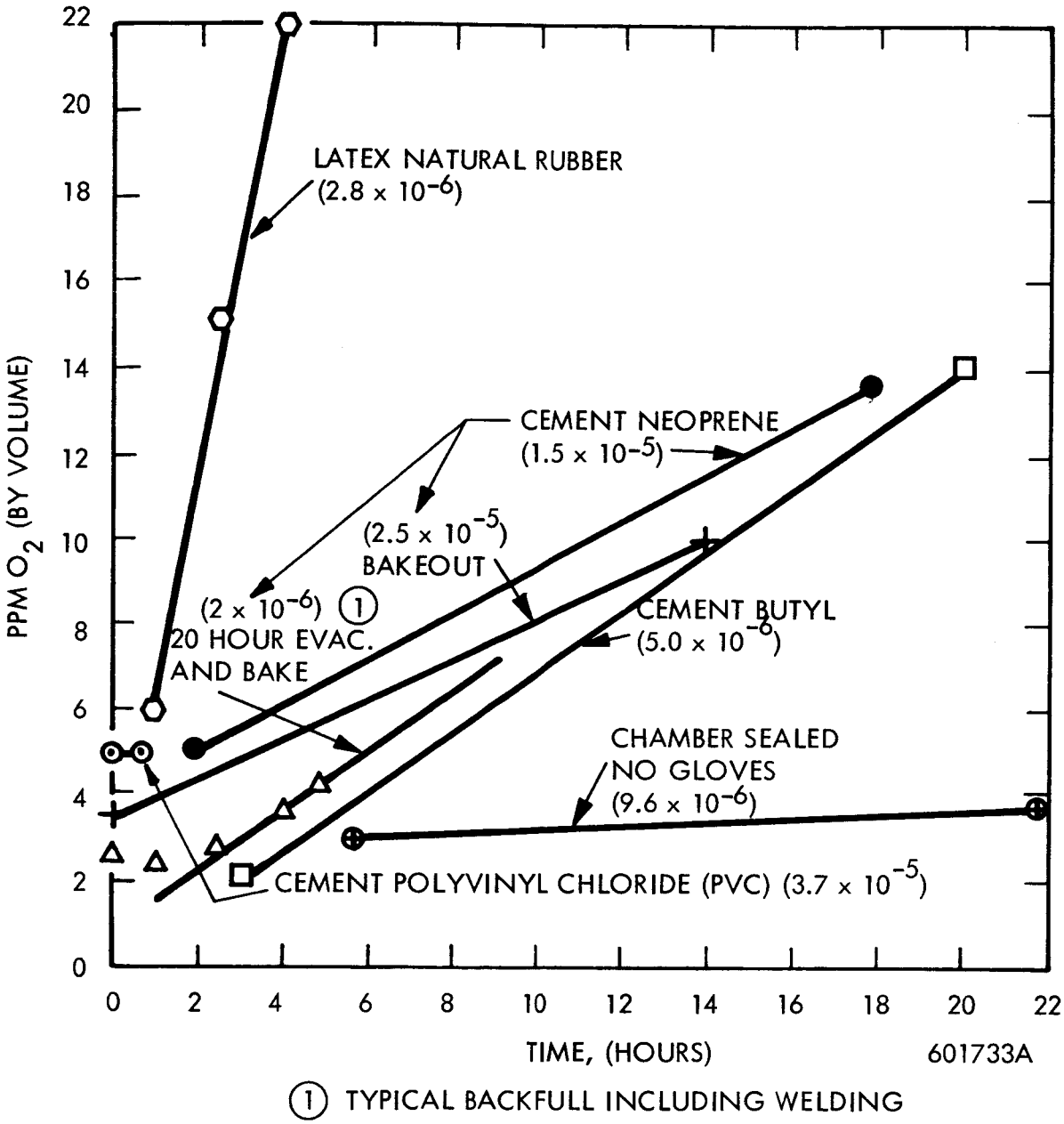

FIGURE 36 - Oxygen Increase With Time in Weld Chamber Atmosphere

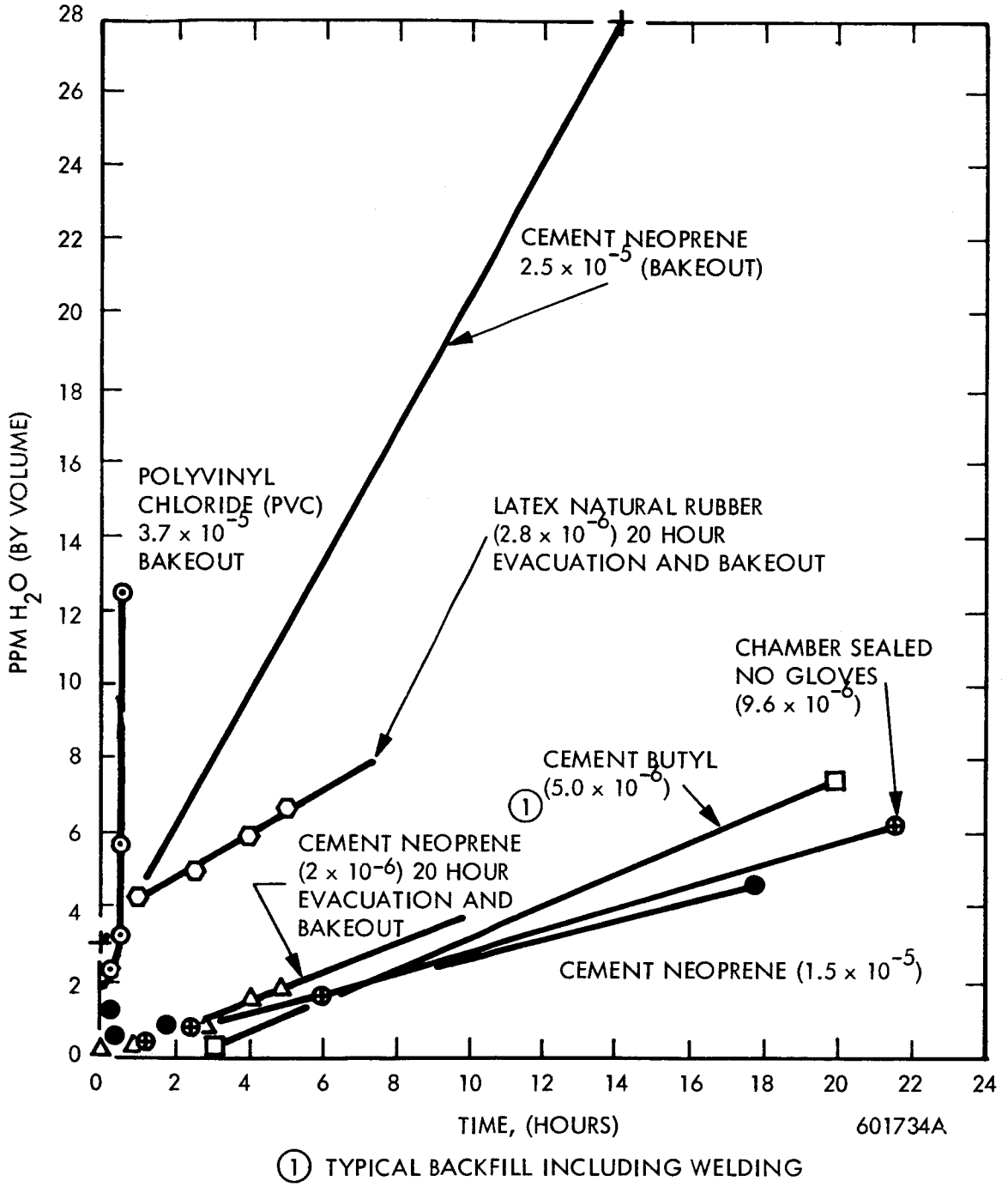

① TYPICAL BACKFILL INCLUDING WELDING

FIGURE 37 - Water Vapor Increase With Time in Weld Chamber Atmosphere

IV. FUTURE WORK

Weld parameter optimization studies will be completed for TIG and EB sheet welds of T-111 and perhaps T-222 if this alloy becomes available. EB parameter studies will be completed for C-129Y and B-66. Preparation of welds for the remainder of the program will be initiated upon selection of the most satisfactory parameters identified in the optimization phase. As these welds are produced, post weld annealing studies will be initiated. TIG welding of the W-25Re and unalloyed tungsten sheet will be undertaken, as time permits, using the recently fabricated weld preheat fixture.

Plate butt welds will be bend tested and welding will be initiated on the second series of these joints.

V. REFERENCES

1. G. G. Lessmann and D. R. Stoner, "Determination of the Weldability and Elevated Temperature Stability of Refractory Metal Alloys", Third Quarterly Report, WANL-PR-(P)-003, NASA CR 54088, December 21 to March 21, 1964.